Available online at www.sciencedirect.com

ScienceDirect

Geochimica et Cosmochimica Acta 72 (2008) 5128–5145

Geochimica et Cosmochimica Acta

www.elsevier.com/locate/gca

Coupled phase and aqueous species equilibrium of the H_2O–CO_2–NaCl–$CaCO_3$ system from 0 to 250 °C, 1 to 1000 bar with NaCl concentrations up to saturation of halite

Zhenhao Duan *, Dedong Li

Key Laboratory of the Earth's Deep Interior, Institute of Geology and Geophysics, Chinese Academy of Sciences, Beijing 100029, China

Received 25 March 2008; accepted in revised form 31 July 2008; available online 14 August 2008

Abstract

A model is developed for the calculation of coupled phase and aqueous species equilibrium in the H_2O–CO_2–NaCl–$CaCO_3$ system from 0 to 250 °C, 1 to 1000 bar with NaCl concentrations up to saturation of halite. The vapor–liquid–solid (calcite, halite) equilibrium together with the chemical equilibrium of H^+, Na^+, Ca^{2+}, $CaHCO_3{}^+$, $Ca(OH)^+$, OH^-, Cl^-, $HCO_3{}^-$, $CO_3{}^{2-}$, $CO_{2(aq)}$ and $CaCO_{3(aq)}$ in the aqueous liquid phase as a function of temperature, pressure, NaCl concentrations, $CO_{2(aq)}$ concentrations can be calculated, with accuracy close to those of experiments in the stated T–P–m range, hence calcite solubility, CO_2 gas solubility, alkalinity and pH values can be accurately calculated. The merit and advantage of this model is its predictability, the model was generally not constructed by fitting experimental data.

One of the focuses of this study is to predict calcite solubility, with accuracy consistent with the works in previous experimental studies. The resulted model reproduces the following: (1) as temperature increases, the calcite solubility decreases. For example, when temperature increases from 273 to 373 K, calcite solubility decreases by about 50%; (2) with the increase of pressure, calcite solubility increases. For example, at 373 K changing pressure from 10 to 500 bar may increase calcite solubility by as much as 30%; (3) dissolved CO_2 can increase calcite solubility substantially; (4) increasing concentration of NaCl up to 2 m will increase calcite solubility, but further increasing NaCl solubility beyond 2 m will decrease its solubility.

The functionality of pH value, alkalinity, CO_2 gas solubility, and the concentrations of many aqueous species with temperature, pressure and $NaCl_{(aq)}$ concentrations can be found from the application of this model. Online calculation is made available on www.geochem-model.org/models/h2o_co2_nacl_caco3/calc.php.

1. INTRODUCTION

H_2O–CO_2–NaCl–$CaCO_3$ system or its subsystems are the most frequently encountered natural fluid systems in and around the Earth. Geochemists often need to calculate such properties as CO_2 gas solubility, calcite solubility, alkalinity and pH values in studies of fluid–rock interactions, secondary porosity in oil reservoir, the precipitation/dissolution of carbonate rocks, the transport-reactive behavior in CO_2 sequestration and so on (Giles, 1987; Giles and de Boer, 1989; Li et al., 2007; Pruess and Spycher, 2007). However, any accurate calculation of the properties mentioned above cannot be done without accurate calculation of coupled phase and aqueous species equilibrium because all of them are complicated functions of temperature, pressure and composition (T–P–m) and all species in different phases are thermodynamically and systematically related. In the liquid phase, the chemical species (H^+, Na^+, Ca^{2+}, $CaHCO_3{}^+$, $Ca(OH)^+$, OH^-, Cl^-, $HCO_3{}^-$, $CO_3{}^{2-}$, $CO_{2(aq)}$ and $CaCO_{3(aq)}$) may associate or dissociate and are directly related to calcite solubility (liquid–solid phase equilibrium), CO_2 solubility (liquid–vapor phase equilibrium), pH values and many other properties. A model of simultaneous calculating coupled phase and aqueous

---

* Corresponding author.
E-mail address: duanzhenhao@yahoo.com (Z. Duan).

0016-7037/$ - see front matter © 2008 Elsevier Ltd. All rights reserved.
doi:10.1016/j.gca.2008.07.025

species equilibrium is essential in accurate calculation of the above properties.

There exist several models or programs for calculating aqueous fluid equilibria including calcite solubility, alkalinity or pH values, such as PHREEQC (Parkhurst and Appelo, 1999), PHRQPITZ (Plummer et al., 1988), WATEQ4F (Ball and Nordstrom, 1991) and MINTEQA2 (Allison et al., 1991). These models or programs find various applications in multiple fields of geochemistry, but none of them are applicable in a large *TPm* range (Fig. 1) with sufficient accuracy because of the experimental data limitation at the time of modeling. PHREEQC yields relatively large error and deviation from experimental data in the calculation of calcite solubility for pressures beyond 100 bar. WATEQ4F can calculate the equilibrium distribution of inorganic aqueous species of major and important minor elements in natural waters, but it is limited below 375.15 K and 100 bar. MINTEQA2 is able to calculate species equilibrium of dilute aqueous solution in the laboratory or in natural aqueous system, but it is also limited below 373.15 K and 100 bar.

There are also some purely empirical methods for calculating solubility of calcite, such as the models of Satman et al. (1999) for the moderate temperature range (from 348 to 523 K) and the models by Caciagli and Manning (2003), Newton and Manning (2002) for supercritical range (above 673 K). These models can only calculate calcite solubility as a function of temperature and pressure in pure water and are limited in the specified range without extrapolation.

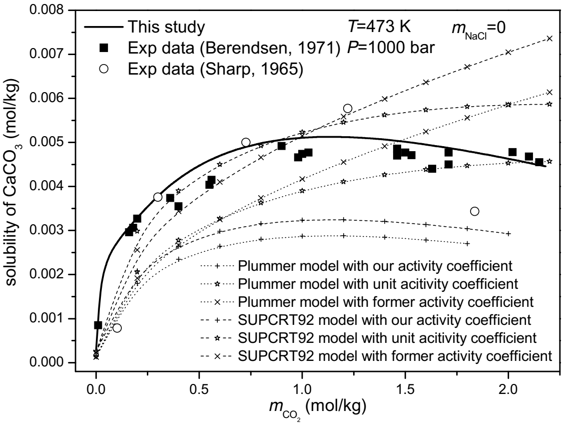

Fig. 1. Solubilities of calcite in aqueous solutions at 473 K and 1000 bar: a comparison of our model (solid line), reported experiments (solid rectangle: Berendsen (1971); circle: Sharp and Kennedy (1965)) and two other popular models. Since the solubilities from all models are dependent on both dissociation constant and activities coefficient, the cross coupling effects of different dissociation constants models (dotted line: Plummer and Busenberg (1982); dash line: SUPCRT92) with activity coefficient models need to be explored. Here we use three kinds of activity coefficient methods: (1) our systemic H_2O–CO_2–NaCl–$CaCO_3$ system activity coefficient model to calculate solubility of calcite directly with results denoted by (+); (2) setting activity coefficient of all species as unit with results denoted by (□); (3) using former activity coefficient model to calculate, and the results are denoted by (×). The results from our dissociation constants and activity coefficient model are the best in agreement with experiments and reveals calcite solubility as a function of CO_2 concentration.

In this study, we develop a thermodynamic model which simultaneously calculates the gas–liquid–solid phase equilibria and chemical species equilibria in the H_2O–CO_2–NaCl–$CaCO_3$ system in a large *TPm* range, hence such geochemically important properties as calcite solubility, CO_2 solubility, pH values and alkalinity can be calculated accurately.

2. PHENOMENOLOGICAL DESCRIPTIONS OF PHASE EQUILIBRIUM AND SPECIES EQUILIBRIUM AS A FUNCTION OF TEMPERATURE, PRESSURE AND COMPOSITION

Potentially two kinds of changes, phase change and chemical species change, may occur in the quaternary system, H_2O–CO_2–NaCl–$CaCO_3$, at a given temperature and pressure. The phase changes alter the mass distribution between vapor, liquid and solid (calcite, halite), and the chemical changes cause the formation or dissociation of H^+, Na^+, Ca^{2+}, $CaHCO_3{}^+$, $Ca(OH)^+$, OH^-, Cl^-, $HCO_3{}^-$, $CO_3{}^{2-}$, $CO_{2(aq)}$ and $CaCO_3{}^0{}_{(aq)}$ in the liquid phase. These changes are complicated functions of temperature, pressure and molality of component, m_{H_2O}, m_{CO_2}, m_{NaCl}, and m_{CaCO_3} (*TPm*). At a given *TPm* condition, the various changes will approach dynamic equilibrium states given sufficient time, though microscopically components still move from one phase to another and species still dissociate or associate to form different species. Geochemically many systems sit there for years or millions of years, so we in many cases can treat them as equilibrium system. Correspondingly, there are two kinds of equilibria, phase equilibrium and chemical species equilibrium, to be described in order to fully understand the diversiform changes of the system under various *TPm* conditions. It is known that at phase equilibrium, the chemical potentials of any component are equal among all phases. For examples, at liquid–vapor phase equilibrium, the chemical potential of CO_2 in the liquid is equal to its chemical potential in the vapor phase; For calcite solubility, $CaCO_3{}^s$ (calcite) ↔ Ca^{2+}+ $CO_3{}^{2-}$, the chemical potential should be equal on both sides. That is

$$\mu_{CaCO_3^s} = \mu_{Ca^{2+}} + \mu_{CO_3^{2-}} \tag{1}$$

where μ_j, is chemical potential defined as

$$\mu_j = \mu_j^0 + RT\ln m_j + RT\ln\gamma_j \text{ (aqueous species)} \tag{2}$$

$$\mu_j = \mu_j^0 + RT\ln x_jP + RT\ln\varphi_j \text{ (vapor species)} \tag{3}$$

where μ_j^0 is standard chemical potential at reference state, which is defined as ideal gas for the vapor phase, or the hypothetical ideal solution at one molar concentration for the liquid phase; m_j and x_j are molality and mole fraction in aqueous phase and vapor phase, respectively. P is vapor pressure. γ_j and φ_j are activity coefficient of species j in liquid phase and fugacity coefficient of species j in vapor phase, respectively. The compositions of all phases at equilibrium are determined by chemical potentials. Therefore, from the definitions above we can see that only standard chemical potentials, fugacity and activity are needed for the calculation of phase equilibrium together with chemical equilibrium.

Specifically, for the calculation of the system equilibrium, we need to (1) identify all possible independent species, phases and chemical reactions; (2) model standard chemical potentials of all species or equilibrium constants of the reactions, since equilibrium constant are related to standard chemical potential, as can be seen later; (3) model non-ideal properties of all species, including activity coefficients and fugacity coefficients as functions of temperature, pressure and composition of the system; (4) find a convergent algorithm to calculate the system equilibrium for a given condition of temperature, pressure and total composition.

2.1. Independent species, phases and chemical reactions

The H_2O–CO_2–NaCl–$CaCO_3$ system may have four possible phases in the *TP* range of this study: vapor phase, liquid phase and two solid phases (halite and calcite). Other solid phases, such as hydrahalite $NaCl{\cdot}2H_2O$, aragonite and gas hydrate are generally outside of the *TP* range of this study.

(1) In vapor phase, there are two kinds of species, CO_2 and H_2O. NaCl and $CaCO_3$ are not considered to be dissolved into vapor in the *TP* range of this study.

(2) In liquid solution, there exist many aqueous species, including H^+, Na^+, Ca^{2+}, $CaHCO_3{}^+$, OH^-, Cl^-, $HCO_3{}^-$, $CO_3{}^{2-}$, $CO_{2(aq)}$ and $CaCO_3{}^0{}_{(aq)}$. The aqueous species $Ca(OH)^+$ is trivial in the $CO_{2(aq)}$ bearing solution because the concentration of OH^- is very low when CO_2 is saturated. So we can assume $Ca(OH)^+$ as fully dissociated (Gimblett and Monk, 1954; Bates et al., 1959; Seewald and Seyfried, 1991) when system reaches vapor–liquid equilibrium. However, when $CaCO_3$ is dissolved in CO_2-free aqueous solution, the concentration of OH^- will increase. In this case, $Ca(OH)^+$ may account for a few percent of total dissolved calcium and is necessary to be considered as a species in order to calculate calcite solubility accurately in various conditions.$CaCl^+{}_{(aq)}$ and $CaCl_{2(aq)}{}^0$ are fully dissociated when temperature goes below 523 K according to Frantz and Marshall (1982), Gillespie et al. (1992), so they can be ignored in the *TP* range of this study. $NaHCO_{3_{aq}}{}^0$ and $NaCO_{3(aq)}{}^-$ are regarded as to be fully dissociated (Nakayama, 1971). $NaCl^0{}_{(aq)}$ is almost completely dissociated in aqueous solutions for temperatures below 523 K. Note that Na^+ and Cl^- tend to be associated as temperatures increases above 573 K (Quist and Marshall, 1968). Thus, we can assume no paired $NaCl^0{}_{(aq)}$ molecules existing in the temperature–pressure range of this study.

(3) Two solid phases, NaCl (halite) and $CaCO_3$ (calcite), are considered in this study. Other solid phases, such as hydrahalite $NaCl{\cdot}2H_2O$ and aragonite and gas hydrate are generally outside of the *TP* range of this study. Calcium carbonate may represent various forms. Calcite is thermodynamically the most stable form in the *T*–*P* range of this study. Aragonite is metastable and can be transformed to calcite. Vaterite is the least stable $CaCO_3$ form, and consequently was not studied thoroughly (Bischoff, 1969; Medeiros et al., 2007). The rate of transformation of aragonite to calcite at 323–373 K is proportional to the square of reaction time in aqueous solution (Bischoff, 1969). Since calcite is the most stable mineral in the *T*–*P* range of this study, we only need to consider calcite as crystal solid of $CaCO_3$. Though other phases, such as aragonite, vaterite, etc, do exist at the temperature ranges of this study and in fact do form and persist for substantial time at these conditions. Their formation and crystallization from aqueous solution are more complex processes where kinetics may play important roles. Because of the limitation of kinetics data, we are not able to further discuss other $CaCO_3$ phases here.

Now we can write the independent reactions among these species or phases. There are 11 possible species (H^+, Na^+, Ca^{2+}, $CaHCO_3{}^+$, $Ca(OH)^+$, OH^-, Cl^-, $HCO_3{}^-$, $CO_3{}^{2-}$, $CO_{2(aq)}$ and $CaCO_3{}^0{}_{(aq)}$ in solution involving independent species equilibrium as expressed by Eqs. (4)–(9)

$$H_2O + CO_{2(aq)} \leftrightarrow HCO_3^- + H^+ \tag{4}$$

$$HCO_3^- \leftrightarrow CO_3{}^{2-} + H^+ \tag{5}$$

$$H_2O \leftrightarrow H^+ + OH^- \tag{6}$$

$$CaHCO_3^+ \leftrightarrow Ca^{2+} + HCO_3^- \tag{7}$$

$$CaCO_3^0 \leftrightarrow Ca^{2+} + CO_3^{2-} \tag{8}$$

$$Ca(OH)^+ \leftrightarrow Ca^{2+} + OH^- \tag{9}$$

In addition, there are four phase equilibrium reactions as follows:

$$H_2O_{(aq)} \leftrightarrow H_2O^g \tag{10}$$

$$CO_{2(aq)} \leftrightarrow CO_2^g \tag{11}$$

$$NaCl^s\ (\text{halite}) \leftrightarrow Na^+ + Cl^- \tag{12}$$

$$CaCO_3^s\ (\text{calcite}) \leftrightarrow Ca^{2+} + CO_3{}^{2-} \tag{13}$$

Other reactions can be derived from the above independent reactions. For example, the liquid solid reaction, $CaCO_3{}^s \leftrightarrow CaCO_3^0$ can be obtained by subtracting Eq. (8) from Eq. (13).

2.2. Equilibrium constants as functions of temperature and pressure

The standard chemical potentials are used to calculate equilibrium constant

$$\ln K_i = -\frac{\Delta G_f^0}{RT} = -\frac{\sum v_j \mu_j^0}{RT} \tag{14}$$

Corresponding to Eqs. (4)–(13), the following equilibrium constants are defined,

$$K_1 = \frac{(m_{\mathrm{H^+}}\gamma_{\mathrm{H^+}}) \cdot (m_{\mathrm{HCO_3^-}}\gamma_{\mathrm{HCO_3^-}})}{a_{\mathrm{CO_2}} \cdot a_{\mathrm{H_2O}}} \tag{15}$$

$$K_2 = \frac{(m_{\mathrm{H^+}}\gamma_{\mathrm{H^+}}) \cdot (m_{\mathrm{CO_3{}^{2-}}}\gamma_{\mathrm{CO_3{}^{2-}}})}{(m_{\mathrm{HCO_3^-}} m_{\mathrm{HCO_3^-}})} \tag{16}$$

$$K_3 = \frac{(m_{\mathrm{H^+}}\gamma_{\mathrm{H^+}}) \cdot (m_{\mathrm{OH^-}}\gamma_{\mathrm{OH^-}})}{a_{\mathrm{H_2O}}} \tag{17}$$

$$K_4 = \frac{(m_{\mathrm{Ca^{2+}}}\gamma_{\mathrm{Ca^{2+}}}) \cdot (m_{\mathrm{HCO_3^-}}\gamma_{\mathrm{HCO_3^-}})}{(m_{\mathrm{CaHCO_3^+}}\gamma_{\mathrm{CaHCO_3^+}})} \tag{18}$$

$$K_5 = \frac{(m_{\mathrm{Ca^{2+}}}\gamma_{\mathrm{Ca^{2+}}}) \cdot (m_{\mathrm{CO_3{}^{2-}}}\gamma_{\mathrm{CO_3{}^{2-}}})}{(m_{\mathrm{CaCO_3^0}}\gamma_{\mathrm{CaCO_3^0}})} \tag{19}$$

$$K_6 = \frac{(m_{\mathrm{Ca^{2+}}}\gamma_{\mathrm{Ca^{2+}}}) \cdot (m_{\mathrm{OH^-}}\gamma_{\mathrm{OH}}^{-})}{(m_{\mathrm{Ca(OH)^+}}\gamma_{\mathrm{Ca(OH)^+}})} \tag{20}$$

$$K_7 = \frac{a_{\mathrm{H_2O_{(g)}}}}{a_{\mathrm{H_2O_{(aq)}}}} = \frac{f_{\mathrm{H_2O_{(g)}}}/P_{\mathrm{tot}}}{a_{\mathrm{H_2O_{(aq)}}}} \tag{21}$$

$$K_8 = \frac{a_{\mathrm{CO_{2(g)}}}}{a_{\mathrm{CO_{2(aq)}}}} = \frac{f_{\mathrm{CO_2^g}}/P_{\mathrm{tot}}}{a_{\mathrm{CO_{2(aq)}}}} \tag{22}$$

$$K_9 = \frac{(m_{\mathrm{Na^+}}\gamma_{\mathrm{Na^+}}) \cdot (m_{\mathrm{Cl^-}}\gamma_{\mathrm{Cl^-}})}{a_{\mathrm{NaCl^s}}} \tag{23}$$

$$K_{10} = \frac{(m_{\mathrm{Ca^{2+}}}\gamma_{\mathrm{Ca^{2+}}}) \cdot (m_{\mathrm{CO_3^{2-}}}\gamma_{\mathrm{CO_3^{2-}}})}{a_{\mathrm{CaCO_3^s}}} \tag{24}$$

These equilibrium constants can be modeled as functions of temperature and pressure.

2.2.1. *Equilibrium constant of species equilibrium (K_1–K_6)*

The equilibrium constants, K_1 and K_2, have been studied by Li and Duan (2007)

$$\begin{aligned} \ln K = {} & a_1 + a_2T + a_3T^{-1} + a_4T^{-2} + a_5\ln T \\ & + (a_6T^{-1} + a_7T^{-2} + a_8T^{-1}\ln T)(P - P_s) \\ & + (a_9T^{-1} + a_{10}T^{-2} + a_{11}T^{-1}\ln T)(P - P_s)^2 \end{aligned} \tag{25}$$

where a_1–a_{11} are parameters (Table 1), P_s is 1 bar at temperatures below 373.15 K or saturation pressure of water at temperatures above 373.15 K.

Marshall and Franck (1981), Quist (1970), Tanger and Pitzer (1989) studied the dissociation constant of pure water (K_3) and established models valid in a wide range of temperature and pressure. In this study, we employ the model of Marshall and Franck (1981) for the dissociation constants of water (K_3) (Appendix A) because it is more reliable in the investigated TP range and accepted by many researchers.

Table 1
The parameters of Eq. (25)

	$\ln K_1$	$\ln K_2$
a_1	233.5159304	−151.1815202
a_2	0.0	−0.088695577
a_3	−11974.38348	−1362.259146
a_4	0.0	0.0
a_5	−36.50633536	27.79798156
a_6	−45.08004597	−29.51448102
a_7	2131.318848	1389.015354
a_8	6.714256299	4.419625804
a_9	0.008393915212	0.003219993525
a_{10}	−0.4015441404	−0.1644471261
a_{11}	−0.00124018735	−0.0004736672395

The three reactions (7)–(9) involve three kinds of calcium species in aqueous solution, $CaHCO_3{}^+$, $CaCO_3{}^0$ and $Ca(OH)^+$. Corresponding to the three reactions, the dissociation constants (K_4, K_5 and K_6) are defined. The dissociation of $CaHCO_3{}^+$ and $CaCO_3{}^0$ was first noted by Greenwald (1941). Many researchers afterwards measured the two dissociation constants (K_4 and K_5) at various temperatures up to 363 K (Neuman et al., 1956; Nakayama, 1968; Martynov et al., 1971; Martynov et al., 1972; Jacobson and Langmuir, 1974; Reardon and Langmuir, 1974; Moore and Verine, 1981; Plummer and Busenberg, 1982; Dorange et al., 1990). Since the experimental data are not sufficient to fit K_4 and K_5 up to 523 K and 1000 bar, we need to find a method to develop a predictive model with good extrapolation for these two constants. Numerous methods have been proposed to predict the dissociation constants for aqueous complexes at temperatures and pressures greater than 298.15 K and 1 bar. These include isocoulombic models (Ruaya, 1988; Gu et al., 1994), density models (Mesmer et al., 1988; Anderson et al., 1991), and various models based on electrostatic theory (Helgeson, 1969; Tanger and Helgeson, 1988; Sverjensky et al., 1997). Most of these models have shown reasonable results based on comparisons between predicted and measured thermodynamic properties. In this study we employed the Sverjensky method to predict the dissociation constants because it has been used successfully in several studies (Shock et al., 1989; Sverjensky et al., 1997; Tanger and Helgeson, 1988).

Three parameters are needed for the calculation of $\log K$ (K_4, K_5) values for dissociation reactions of the two complexes, $CaHCO_3{}^+$ and $CaCO_3{}^0$: (1) the apparent standard free energy of formation of each species at the reference temperature and pressure (298.15 K and 1 bar); (2) the standard partial molal entropy of each complex at the reference TP condition; (3) the heat capacity of each complex at the reference TP condition. The details of the thermodynamic equations and parameters are presented in the Sverjensky paper (Sverjensky et al., 1997). The overall equation used to calculate $\log K$ for each complex as a function of pressure and temperature is given by

$$\log K = \frac{1}{2.303RT}\left\{\begin{array}{l} -\sum\limits_i n_i\Delta_f\overline{G}^0_{i,T} + \Delta_f\overline{G}^0_{P_r,T_r} - \overline{S}^0_{P_r,T_r}(T - T_r) \\ -\left[0.6087\overline{C}^0_{P_r,T_r} - \omega_{P_r,T_r}T_rX_{P_r,T_r} + 5.85\right]f_1(T) \\ -\left[2037\overline{C}^0_{P_r,T_r} - 30460\right]f_2(T) + \omega_{P_r,T_r}f_3(P,T) \\ \quad +f_4(P,T) \end{array}\right\} \tag{26}$$

where n_i and $\Delta_f\overline{G}^0_{i,T}$ refer to the stoichiometric coefficients in the dissociation reactions and the free energies of formation for species ($HCO_3{}^-$, $CO_3{}^{2-}$ and Ca^{2+}) other than $CaHCO_3{}^+$ and $CaCO_3{}^0$ in each reaction. Functions f_1 to f_4 in Eq. (26) are defined by the following Eqs. (27)–(30) (Sverjensky et al., 1997):

$$f_1(T) = T\ln\left(\frac{T}{T_r}\right) - T + T_r \tag{27}$$

$$f_2(T) = \left[\left(\frac{1}{T-\theta}\right) - \left(\frac{1}{T_r-\theta}\right)\right] \times \left(\frac{\theta - T}{\theta}\right) - \frac{T}{\theta^2}\ln\left[\frac{T_r(T-\theta)}{T(T_r-\theta)}\right] \tag{28}$$

$$f_3(P,T) = \left[\frac{1}{\varepsilon} - \frac{1}{\varepsilon_{P_r,T_r}} + Y_{P_r,T_r}(T - T_r)\right] \tag{29}$$

$$f_4(P,T) = k[\omega - \omega_{P_r,T_r}]\left(\frac{1}{\varepsilon} - 1\right) \tag{30}$$

where k stands for a switch constant which is equal to unity for ionic aqueous species and to zero for neutral aqueous species. ω and $\omega_{Pr,Tr}$ in Eqs. (26) and (30) are the conventional Born coefficients for charged aqueous species. $\Delta_f\overline{G}^0_{P_r,T_r}$, $\overline{S}^0_{P_r,T_r}$, $\overline{C}^0_{P_r,T_r}$ and ω_{P_r,T_r} for species of $CaHCO_3{}^+$ and $CaCO_3{}^0$ were optimized simultaneously by minimizing the residuals between calculated and experimental $\log K$ values using a simplex algorithm (Nelder and Mead, 1965). This was done conveniently using the Matlab© programming platform. The residual function is defined as the sum of the squares of the difference between experimental and calculated $\log K$ values. The regressed standard state thermodynamic properties and parameters are compiled in Table 2. The values for $CaHCO_3{}^+$ and $CaCO_3{}^0$ from SUPCRT92 Johnson et al. (1992), Sverjensky et al. (1997) are also listed for comparison.

2.2.2. Liquid–vapor phase equilibrium (K_7, K_8)

In the quaternary system H_2O–CO_2–NaCl–$CaCO_3$ below 523 K, the amount of NaCl and $CaCO_3$ entering the vapor phase is trivial and negligible. We only need to consider the liquid–vapor equilibrium of CO_2 and H_2O. The equilibrium constants are defined by Eqs. (21) and (22). For the distribution of H_2O between liquid and vapor (K_7),

$$H_2O^{(V)} \leftrightarrow H_2O^{(L)} \tag{31}$$

$$\hat{f}^{(V)}_{H_2O} = \hat{f}^{(L)}_{H_2O} \tag{32}$$

or

$$y_{H_2O}\hat{\phi}^{(V)}_{H_2O}P = x_{H_2O}\gamma_{H_2O}\phi^{sat}_{H_2O}P^{sat}_{H_2O}(PF)_{H_2O} \tag{33}$$

The water content in vapor phase can be calculated by following formula.

$$y_{H_2O} = x_{H_2O}\gamma_{H_2O}\phi^{sat}_{H_2O}(P^{sat}_{H_2O}/P) \cdot [(PF)_{H_2O}/\hat{\phi}^{(V)}_{H_2O}] \tag{34}$$

where y_{H_2O} is H_2O content in vapor phase, x_{H_2O} and γ_{H_2O} are H_2O mole fraction and activity coefficient in the aqueous liquid, respectively. The activity of water in the liquid solution, $a_{H_2O} = x_{H_2O} \cdot \gamma_{H_2O}$, can be calculated by the Pitzer model. $\phi^{sat}_{H_2O}$ is fugacity coefficient of saturated water, and it can be calculated by equation of state of pure water (Duan et al., 1992). $P^{sat}_{H_2O}$ is saturation pressure of water calculated by IAPWS-IF97 (Wagner and Kruse, 1998). $(PF)_{H_2O}/\hat{\phi}^{(V)}_{H_2O}$ is the ratio of Poynting Factor to the vapor-phase fugacity coefficient of H_2O at liquid–vapor coexisting state. It is a function of temperature and pressure.

$$(PF)_{H_2O}/\hat{\phi}^{(V)}_{H_2O} = F(T,P) \tag{35}$$

We used the experimental data in gas phase for the H_2O–CO_2 system to obtain an empirical equation for computing the ratio (Blencoe et al., 2001; Spycher et al., 2003). Spycher et al. summarized experimental data of water content in vapor phase, which are used to fit the empirical equations with an average deviation of 5–10% and maximum deviation of 20% for the water content in the vapor. The formula and parameters for calculation of Eq. (35) are listed in Table 3. Substituting the results in Eq. (35) into Eq. (34), the water content in the vapor phase can be calculated.

Based on the definition of K_8 in Eq. (22), the equilibrium constant can be re-written as:

$$\begin{aligned} \ln K_8 &= \ln f_{CO_2^g} - \ln a_{CO_{2(aq)}} = \ln P_{CO_2} - \ln m_{CO_2} \\ &\quad + \ln \varphi_{CO_2} - \ln \gamma_{CO_2} \\ &= \ln k_H + PF \end{aligned} \tag{36}$$

where k_H is Henry's constant which is defined by

$$k_H = \lim_{P \to P_s} f_{CO_2}/m_{CO_2}(T,P) \tag{37}$$

Table 3
The calculation of Eq. (35)

The range of pressure in bar	$\ln[(PF)_{H_2O}/\hat{\phi}^{(V)}_{H_2O}] =$
$\ln P \leqslant 4.0$	$A + B\ln P + C(\ln P)^2$
$\ln P \geqslant 5.0$	$D + E\ln P$
$4.0 < \ln P < 5.0$	$d_1 + d_2\ln P + d_3(\ln P)^2 + d_4/\ln P$

$A = -20.7600738043549 + 0.08978033008 11T - 0.0000954680712T^2$
$B = 3.08284 - 0.00956T + 0.0000092069T^2$
$C = -0.38986 + 0.00228T - 0.0000026679T^2$
$D = -6.6623328249993 - 0.057517079835T + 0.0000643503862T^2$
$E = -0.445272747863 + 0.0130486543901T - 0.000015177905T^2$

$d_4 = -(2.0M - 2.0N + P + Q)/0.0025$	$M = A + 4B + 16C$
$d_3 = (Q - P - 0.0225d_4)/2.0$	$N = D + 5E$
$d_2 = P - 8.0d_3 + d_4/16.0$	$P = B + 8C$
$d_1 = M - 4.0d_2 - 16.0d_3 - d_4/4.0$	$Q = E$

Note: T in K, P in bar.

Table 2
Standard partial molal properties at 25 °C for $CaCO_{3(aq)}{}^0$and $CaHCO_3{}^+$ complexes regressed from experimentally derived constants

	$CaHCO_3{}^+$ this study	$CaHCO_3{}^+$ (DPRONS96.DAT)	$CaCO_{3(aq)}{}^0$ this study	$CaCO_{3(aq)}{}^0$ Sverjensky et al. (1997)
$\Delta_f\overline{G}^0_{P_r,T_r}$ (cal mol^{-1})	−273841.0	−273830	−262695.0	−262850
$\overline{S}^0_{P_r,T_r}$ (cal mol^{-1} K^{-1})	28.624	16.00	2.7188	2.5
$\overline{C}^0_{P_r,T_r}$ (cal mol^{-1} K^{-1})	−25.4118	56.9	5.2175	−29.6
$\omega_{P_r,T_r} \times 10^{-5}$ (cal mol^{-1})	0.11026	0.3084	17.826	−0.038

where P_s is saturated pressure of water in bar at various temperatures. PF is Poynting Factor defined by:

$$PF = \int_{P_s}^{P} \widetilde{V_m} \mathrm{d}P/RT \tag{38}$$

where R is the gas constant, T is temperature in Kelvin, $\widetilde{V_m}$ is partial molar volume of $CO_{2(aq)}$. Generally the partial molar volume varies with composition as following

$$\widetilde{V}_m = \left(\frac{\partial V}{\partial n_m}\right)_{p,T,n'} \tag{39}$$

where V is total volume of the aqueous solution which can be accurately calculated as a function of temperature, pressure and composition (Duan et al., 2008). In this study, we employed a concise method for $\widetilde{V}_m$ which can be calculated by following equation (Garcia, 2001)

$$\widetilde{V}_m = 66.44783 + 0.285006T + 0.0006308T^2 \tag{40}$$

where T is temperature in K. The original Eq. (40) is in °C, we recalculated the equation with unit K.

2.2.3. Halite and calcite solubility (K_9, K_{10})

In order to calculate the solubility of halite and calcite (K_9, K_{10}) of Eqs. (12) and (13), we need to calculate the standard chemical potential of $NaCl^s$ and $CaCO_3^s$ as a function of temperature and pressure. These are taken from SUPCRT92 (Johnson et al., 1992) since it was based on extensive experimental data for these two minerals. They are consistent with the model of Harvie et al. (1984) for these two minerals at water saturation pressure, but more reliable at higher pressures. In this study, we combine the standard chemical potentials of Na^+, Cl^- and halite as equilibrium constant K_9 and obtain a TP function of K_9 which is written out in appendix B.

2.3. Non-ideal properties of species

The chemical potentials at reference states can be equivalently calculated from the equilibrium constants discussed above. However, adding NaCl, $CaCO_3$ or CO_2 in the system will change the chemical potential of all the species involved and can lead to deviations from the reference states. The deviation is a function of temperature, pressure and composition which can be expressed by fugacity coefficient for vapor species and activity coefficient for aqueous species. For solid species, we can set the activity coefficient as unit because the solids are pure substances whose activity is equal to 1.

2.3.1. The fugacity coefficient of vapor species

The fugacity coefficient of CO_2, ϕ_{CO_2}, can be calculated from the EOS of Duan et al. (1992). The water fugacity coefficient in vapor phase has been combined into Eq. (35).

2.3.2. The activity coefficients of aqueous species

Since 1973, Pitzer and co-workers established a specific interaction model which has been used to estimate the activity coefficients of chemical species in solutions up to high concentrations (Pitzer, 1973; Pitzer and Mayorga, 1973; Pitzer and Kim, 1974). This model has been applied to compute activity coefficient in high concentrated electrolytic solutions successfully (Harvie and Weare, 1980; Harvie et al., 1984). In this study, we employed the Pitzer model to calculate activity coefficients of species in aqueous solution. The Pitzer equations have been discussed in detail in many publications. Here, we only need to determine the Pitzer parameters, $\beta^{(0)}_{MX}$, $\beta^{(1)}_{MX}$, $\beta^{(2)}_{MX}$, and C^{φ}_{MX} for each cation–anion pair, θ_{ij} for each cation–cation or anion–anion pair; ψ_{ijk} for each cation–cation–anion and anion–anion–cation triplet, λ_{ni} for ion-neutral pairs, and ζ_{nij} for neutral–anion–cation triplet. These parameters are functions of temperature. The parameters for each cation–anion pair are functions of temperature and pressure. Though most of Pitzer parameters of the H_2O–CO_2–NaCl–$CaCO_3$ system can be obtained from previous publications Harvie et al. (1984), Christov and Møller (2004b), some parameters need to be re-evaluated. In this study only the neutral component in aqueous solution ($CO_{2(aq)}$) interactive parameters were be revaluated and other important parameters were obtained from previous literature. All other unmentioned parameters are set to zero.

Recently, Li and Duan (2007) studied the activity coefficients of all possible species using Pitzer equations in the system of H_2O–CO_2–NaCl. This study evaluated the new parameters of calcium interaction in aqueous solution (Table 4). The virial constants, $\beta^{(0)}_{Ca-CO_3}\beta^{(1)}_{Ca-CO_3}$ $\beta^{(2)}_{Ca-CO_3}C^{\varphi}_{Ca-CO_3}$, $\beta^{(0)}_{CaHCO_3-Cl}\beta^{(1)}_{CaHCO_3-Cl}C^{\varphi}_{CaHCO_3-Cl}$ and so on contribute very little to the activity coefficient, because these species concentrations are generally less than 0.001 m due to their small dissociation constants of calcium carbonate (K_5 and K_{10}). Therefore, we can set these parameters to zero. The virial coefficients, θ's and ψ's, are in general independent on pressure. Other researchers also reported a very small dependence of pressure for mixing parameters in the system Na–K–Mg–Cl–SO_4–OH (Pabalan and Pitzer, 1987). In this study, we take account of the major calcium species in aqueous solution, Ca^{2+}, $Ca(OH)^+$, ${CaHCO_3}^+$ and ${CaCO_{3(aq)}}^0$ Since the concentration of ${CaCO_{3(aq)}}^0$ is very low, its contribution to the activity coefficient is negligible. However, the effect from the neutral component, CO_2 can be substantial in aqueous solution and the parameters λ_{CO_2-Ca} and $\lambda_{CO_2-CaHCO_3}$ must be determined. In order to obtain the two parameters in the TP range of this study, we need to review the experimental solubility of calcite in CO_2 and NaCl aqueous solutions.

2.3.3. Experimental data on calcite solubility in CO_2 + NaCl aqueous solution

The solubility of $CaCO_3$ in water depends on the presence of CO_2, the concentration of which is a function of temperature, pressure and molality of NaCl. Since the 19th century, a voluminous literature bearing on the solubility of $CaCO_3$ has accumulated (Fresenius, 1846; Lassaigne, 1848). Miller (1952) summarized most of the early data and carried out the first thorough experimental study at temperatures up to 373.15 K. After that many researchers reported calcite solubilities in aqueous solution or in NaCl aqueous solutions (Table 5). These data can be classified into moderate pressure data and high pressure data. The high pressure experimental data include Berendsen (1971), Malinin

Table 4
All calcium-relative parameters of Pitzer equations

$\beta^{(0)}_{\text{Ca–OH}}\beta^{(1)}_{\text{Ca–OH}}C^{\varphi}_{\text{Ca–OH}}$		Christov and Møller (2004a), Harvie et al. (1984)	
$\beta^{(0)}_{\text{Ca–Cl}}\beta^{(1)}_{\text{Ca–Cl}}C^{\varphi}_{\text{Ca–Cl}}$		Christov and Møller (2004a), Greenberg and Møller (1989)	
$\beta^{(0)}_{\text{Ca–HCO}_3}\beta^{(1)}_{\text{Ca–HCO}_3}C^{\varphi}_{\text{Ca–HCO}_3}$		—	
$\beta^{(0)}_{\text{Ca–CO}_3}\beta^{(1)}_{\text{Ca–CO}_3}\beta^{(2)}_{\text{Ca–CO}_3}C^{\varphi}_{\text{Ca–CO}_3}$		—	
$\beta^{(0)}_{\text{CaHCO}_3\text{–OH}}\beta^{(1)}_{\text{CaHCO}_3\text{–OH}}C^{\phi}_{\text{CaHCO}_3\text{–OH}}$		—	
$\beta^{(0)}_{\text{CaHCO}_3\text{–Cl}}\beta^{(1)}_{\text{CaHCO}_3\text{–Cl}}C^{\phi}_{\text{CaHCO}_3\text{–Cl}}$		—	
$\beta^{(0)}_{\text{CaHCO}_3\text{–HCO}_3}\beta^{(1)}_{\text{CaHCO}_3\text{–HCO}_3}C^{\phi}_{\text{CaHCO}_3\text{– HCO}_3}$		—	
$\beta^{(0)}_{\text{CaHCO}_3\text{–CO}_3}\beta^{(1)}_{\text{CaHCO}_3\text{–CO}_3}\beta^{(2)}_{\text{CaHCO}_3\text{–CO}_3}C^{\phi}_{\text{CaHCO}_3\text{–CO}_3}$		—	
$\theta_{\text{H-Ca}}$	Christov and Møller (2004a)	$\theta_{\text{Na-Ca}}$	—
$\psi_{\text{H-Ca-OH}}$	—	$\psi_{\text{Na-Ca-OH}}$	—
$\psi_{\text{H-Ca-Cl}}$	Christov and Møller (2004a)	$\psi_{\text{Na-Ca-Cl}}$	—
$\psi_{\text{H–Ca–HCO}_3}$	—	$\psi_{\text{Na–Ca–HCO}_3}$	—
$\psi_{\text{H–Ca–CO}_3}$	—	$\psi_{\text{Na–Ca–CO}_3}$	—
$\psi_{\text{Ca-OH-Cl}}$	Christov and Møller (2004a)	$\psi_{\text{Ca–OH–HCO}_3}$	—
$\psi_{\text{Ca–OH–CO}_3}$	—	$\psi_{\text{Ca–Cl–HCO}_3}$	—
$\psi_{\text{Ca–Cl–CO}_3}$	—	$\psi_{\text{Ca–HCO}_3\text{–CO}_3}$	—
$\lambda_{\text{CO}_2\text{–Ca}}$	This study	$\lambda_{\text{CO}_2\text{–CaHCO}_3}$	This study

Note: —, set to zero in this study.

Table 5
Measurements of calcite solubility after 1950

Authors	System	*T*	*P*	N^a
Miller (1952)	$CaCO_3$–H_2O–CO_2–NaCl 0–0.5 mol/kg	0–104 °C	1–100 bar	188
Weyl (1959)	$CaCO_3$–H_2O–CO_2	10–70 °C	1 bar	40
Ellis (1959, 1963)	$CaCO_3$–H_2O–CO_2–NaCl 0–1.0 mol/kg	98–320 °C	0.97–62.9 bar	107
Segnit et al. (1962)	$CaCO_3$–H_2O–CO_2	75–200 °C	2–60 bar	263
Morey (1962)	$CaCO_3$–H_2O	25–350 °C	200 bar	10
Sharp and Kennedy (1965)	$CaCO_3$–H_2O–CO_2	200–600 °C	42–1433 bar	90
Berendsen (1971)	$CaCO_3$–H_2O–CO_2	100–300 °C	100–1000 bar	107
Malinin and Kanukov (1971)	$CaCO_3$–H_2O–CO_2–NaCl 1–3 mol/kg	200–600 °C	600–1000 bar	101
Plummer and Busenberg (1982)	$CaCO_3$–H_2O–CO_2	0–90 °C	1 bar	141
Sass et al. (1983)	$CaCO_3$–H_2O–CO_2	25 °C	1 bar	59
Pool et al. (1987)	$CaCO_3$–H_2O–CO_2–NaCl 1–4.7%	100–300 °C	135 bar 1900–2000 psi	114
Nagy (1988)	$CaCO_3$–H_2O–NaCl 0.4–5.6 mol/kg	25–89 °C	1 bar	98
Wolf et al. (1989)	$CaCO_3$–H_2O–CO_2–N_2–NaCl 0–6.24 mol/kg	10–60 °C	1 bar 0.0076–0.0095 bar P_{CO_2}	42

Note: ^{a}Number of measurements.

and Kanukov (1971), Sharp and Kennedy (1965). Under these *TP* conditions, CO_2 is unsaturated in aqueous solution, and no vapor coexisting with liquid phase. Thus, the concentration of CO_2 in solution is variable and cannot be determined by its solubility. Berendsen (1971), Sharp and Kennedy (1965) reported calcite solubility data in aqueous CO_2 solutions, and Malinin and Kanukov (1971) reported that in aqueous CO_2–NaCl solutions. Others

Table 6
The neutral-ion parameters of CO_2 for Eq. (41)

	$\lambda_{\text{CO}_2\text{–Ca}}$	$\lambda_{\text{CO}_2\text{–CaHCO}_3}$
a_1	−6.81373167	1.32300207
a_2	8.479439e−3	−1.169756e−3
a_3	−6.71	−10.5650328
a_4	517.21408651092	−103.85163
a_5	1.169219e−3	−9.67235e−5
a_6	1.88544e−6	−2.3244e−8

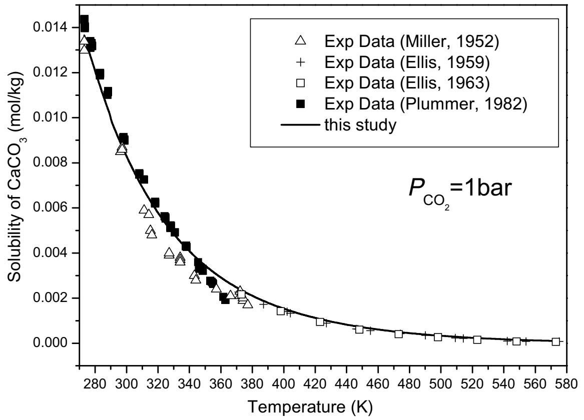

Fig. 2. The solubility of calcite at temperature from 273 to 573 K and 1 bar CO_2 partial pressure. The total pressure of system is the sum of CO_2 partial pressure and water vapor-saturated pressure which can be found from this model. The solid curve is calcite solubilities from this model.

published many sets of experimental data with CO_2 saturated, and the quaternary system can be at vapor–liquid–solid phase equilibrium. Ellis (1959) reported calcite solubility data at vapor–liquid boundary, Ellis (1963) later reevaluated and revised these data. Segnit et al. (1962) reported another set of experimental data independently in the same *TP* range (348–473 K and 2–60 bar), which are in good agreement with those of Ellis. These data are used for the parameterization in this study. In the low *TP* range (273.15–373.15 K and around 1 bar), there exist many published experimental data.

λ_{CO_2-Ca} and $\lambda_{CO_2-\ CaHCO_3}$ as temperature and pressure are evaluated by fitting experimental calcite solubility data together with chemical reaction equilibrium constant and Pitzer activity coefficient. The CO_2–ion interaction parameters can be described by

$$\lambda_{CO_2-i} = a_1 + a_2T + a_3/(T-210) + a_4/(P+100) + a_5T\log(P) + a_6T(P-75)\log(P) \quad (41)$$

where *i* denotes Ca^{2+} or $CaHCO_3{}^{+}$. All parameters (a_1–a_6) in Eq. (41) were optimized simultaneously by minimizing the residuals between calculated and measured solubility data. Conventional residual function is Eq. (42)

$$S = \sum_{i=1}^{n}(\mathrm{m}_{i,\text{measured}} - \mathrm{m}_{i,\text{calculated}})^2 \quad (42)$$

where *S* is residual value, $m_{i,\text{measured}}$ and $m_{i,\text{calculated}}$ are the *i*th measured and calculated calcite solubility, respectively.

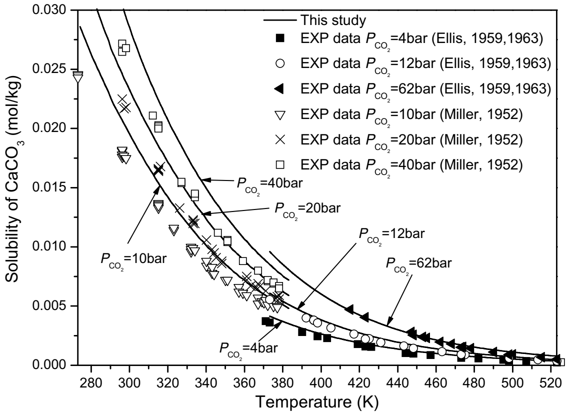

Fig. 3. The solubility of calcite from 273 to 523 K and CO_2 partial pressure from 4 to 62 bar. The total pressure is sum of water vapor-saturated pressure and CO_2 partial pressure. The solid curve is calculated using this model. Comparisons are shown with experimental data.

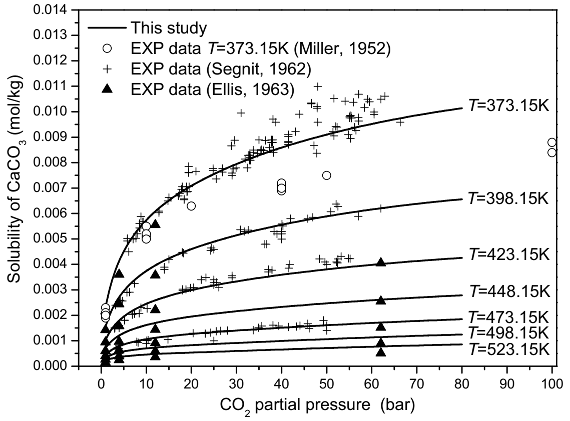

Fig. 4. Calculated calcite solubilities as a function of CO_2 partial pressure are compared with experimental data at different temperatures. The solid lines are calculated using this model which need four independent variable values (temperature, total pressure, total CO_2 concentration and NaCl concentration) as input condition. The total pressure is sum of water vapor-saturated pressure and CO_2 partial pressure. Total CO_2 concentration includes dissociated CO_2 and undissociated CO_2 in aqueous solution.

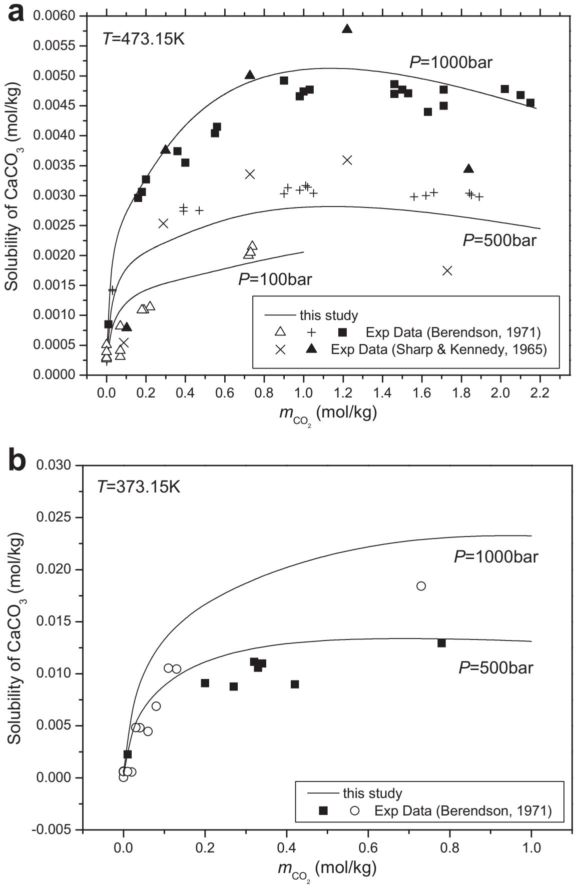

Fig. 5. Calculated calcite solubilities as a function of CO_2 molality as compared with experimental data at different temperatures (a, 473.15 K and b, 373.15 K). The different dots and cross are experimental data from Berendsen (1971); Sharp and Kennedy (1965), respectively. We can find that this model can repeat the experimental data at 473.15 K within experimental deviation of about 10%. Because of the lack of experimental data (only one exp point), we cannot confirm the reliability of the data point at 373.15 K and 1000 bar. From this figure, we see that the solubilities of calcite will decrease with CO_2 molality increasing in the high range of CO_2 molality (above 1.0 mol/kg) at high temperature and high pressure (it is necessary because only high pressure can bring high molality of CO_2 in aqueous solution).

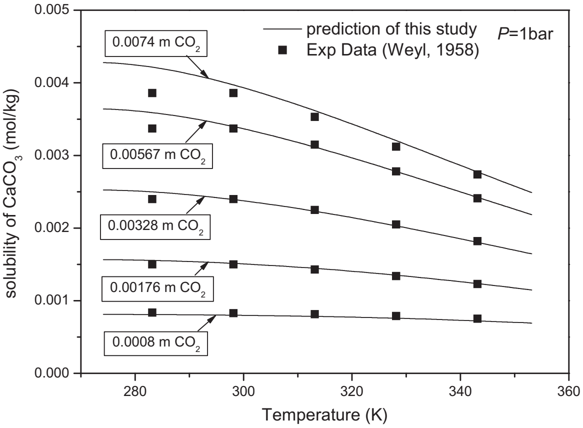

Fig. 6. Calculated calcite solubilities as a function of temperature are compared with experimental values at different CO_2 molalities at moderate pressure.

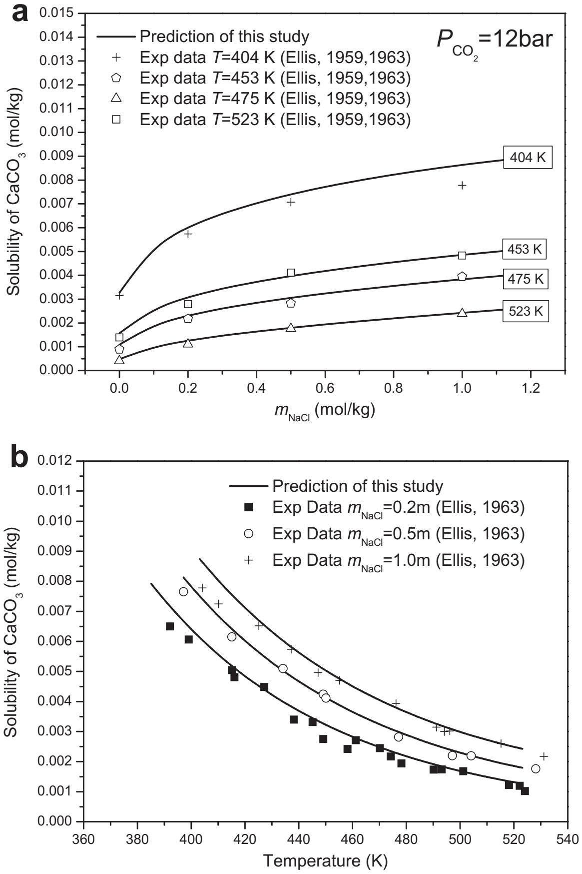

Fig. 7. (a) Calculated calcite solubilities as a function of NaCl molalities are compared with experimental values at different temperature at fixed CO_2 partial pressure (12 bar). In this case, the vapor of CO_2 will coexist with the aqueous solution, but the $CO_{2(aq)}$ concentration is variable with temperature and NaCl concentration. (b) Calculated calcite solubilities as a function of temperature as compared with experimental values at different concentration of NaCl at fixed CO_2 partial pressure (12 bar). This model agrees with experimental data from Ellis (1963), which shows that the model successfully predict the solubilities of calcite in various NaCl solutions even these data are not used in the parameterization.

Due to the large fluctuating calcite solubility (10^{-4}–10^{-2} mol/kg) under various conditions (T–P–m_{CO_2}), we use the logarithm in the minimization. Thus, the residual function to be minimized is defined as:

$$S = \sum_{i=1}^{n} [\log(m_{i,\text{measured}}) - \log(m_{i,\text{calculated}})]^2 \qquad (43)$$

In this process, the calcite solubilities are calculated in the method of coupled phase and aqueous species equilibrium. The computing details will be discussed in the next section. Using the analogous regression methods described above, we obtained the parameters of Eq. (41) as listed in Table 6. In this study, we only use the data of CO_2–H_2O–$CaCO_3$ system in the fitting, and the data in the CO_2–H_2O–NaCl–$CaCO_3$ system are not used. As we will see in next section, the accurate reproducing of the calcite solubility data in the CO_2–H_2O–NaCl–$CaCO_3$ system demonstrates the excellent predictability of this model.

2.4. Algorithm for simultaneous calculating coupled phase and aqueous species equilibrium

Since equilibrium constants (or standard chemical potentials) are functions of temperature and pressure, and fugacity and activity are functions of temperature, pressure and composition, a non-linear algorithm is needed to solve for coupled phase and aqueous species equilibrium in the quaternary system In this work we employed the revised EQBRM code (Anderson and Crerar, 1993) to calculate the concentrations of all aqueous species in a system equilibrium. Vapor (CO_2), solid halite ($NaCl^s$) and solid $CaCO_3{}^s$ calcite are considered as special species in the program.

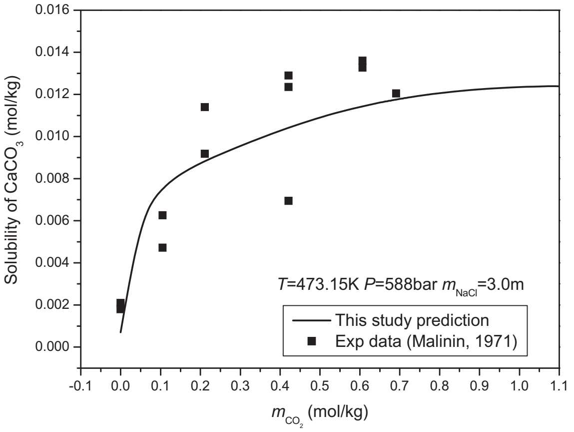

Fig. 8. Calcite solubility in various m_{NaCl} solutions predicted by this model as compared with experimental data from Malinin and Kanukov (1971) in the high TPm_{NaCl} range (473.15 K, 588 bar and 3.0 m NaCl). In this range, the experimental data are rare and are scattered.

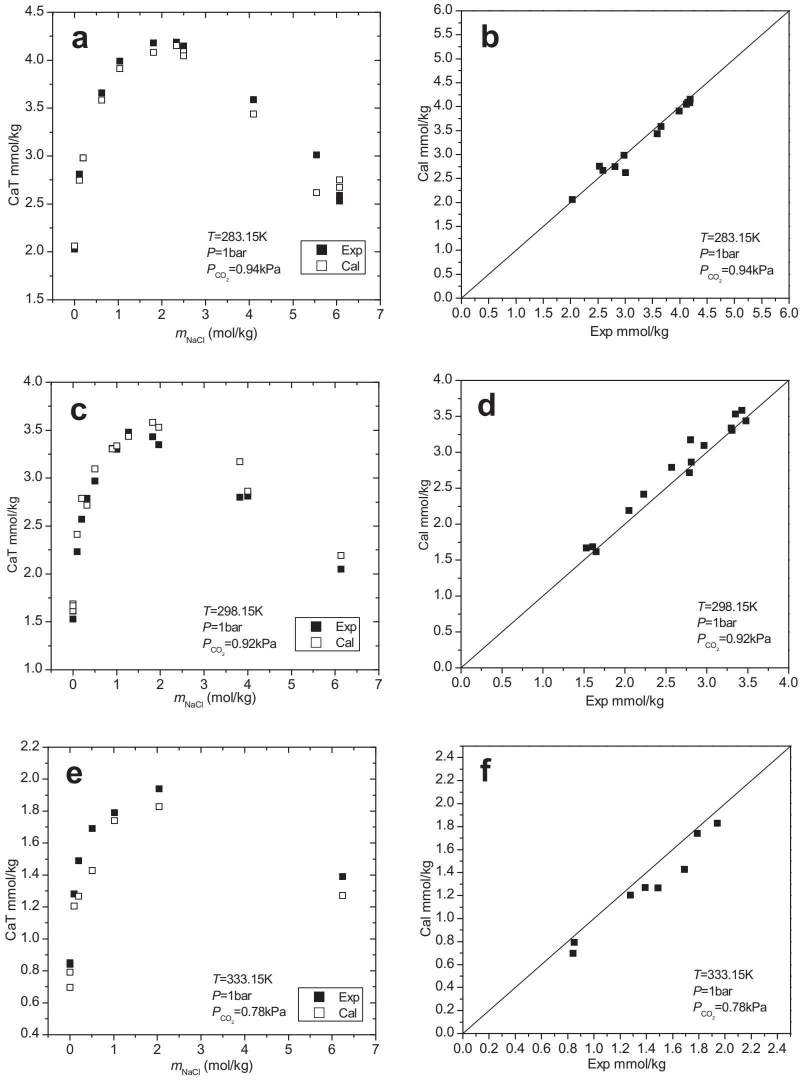

Fig. 9. Comparison between total calcium content (CaT) in solution of this model's prediction and those of experimental data from Wolf et al. (1989). We employed total carbon dioxide content ($\sum CO_2$) from their experiment as input at every point for calculation. (a, c and e) Well agreement between model's calculation and experimental data at 283.15, 298.15 and 333.15 K. (b, d and e) The ratio between calculated value and experimental value. We can find the ratio is near to unit with little variation (average <5%) at the three temperature condition. Moreover, we can predict the relation between solubility of calcite and concentration of NaCl in aqueous solution. In any temperature, solubility of calcite will reach a max value at the NaCl concentration of about 2.0 m.

3. CALCULATION OF CALCITE SOLUBILITY, HALITE SOLUBILITY, CO_2 SOLUBILITY, ALKALINITY AND PH

3.1. Calcite solubility

The calcite solubility data can be classified into two categories, those with CO_2 saturated and those with CO_2 unsaturated. The experimental data with CO_2 saturated include: those of Ellis (1959, 1963), Miller (1952), Plummer and Busenberg (1982), Segnit et al. (1962), Wolf et al. (1989) (2) and the data with CO_2 unsaturated include the data reported by Berendsen (1971), Malinin and Kanukov (1971), Nagy (1988), Pool et al. (1987), Sharp and Kennedy (1965), Weyl (1959).

3.1.1. H_2O–CO_2–$CaCO_3$ system

Ellis(1959, 1963), Miller (1952), Plummer and Busenberg (1982) reported the experimental data with partial pressure of CO_2 of 1 bar and temperature from 273.15 to 573.15 K. As shown in Fig. 2 that our model is in general in good agreement with most of the experimental data. Except for the temperature range of 340–373 K, the model prediction is a little above the experimental data of Miller (1952), Plummer and Busenberg (1982). This should be understandable since the experimental data were measured at pressures below 1 bar. Under elevated P_{CO_2} conditions, our model also reproduces most of the experimental data (Miller, 1952; Ellis, 1959, 1963; Segnit et al., 1962), as displayed in Fig. 3. Ellis (1963), Segnit et al. (1962) reported experimental data up to high temperatures and P_{CO_2} up to 65 bar. As can be seen from Fig. 4 that these data are well reproduced by this model, except for a few points of Miller's data, which is obviously inconsistent with other data points.

The solubility of calcite has also been measured in CO_2 unsaturated aqueous solutions (Sharp and Kennedy, 1965; Berendsen, 1971). As shown in Figs. 5 and 6, these experimental data are generally well predicted by the model of this study even under very high pressures.

3.1.2. H_2O–CO_2–NaCl–$CaCO_3$ system

Adding NaCl in the aqueous solution will inevitably affect the activity of all species in the solution, including all the calcium species, thus affecting the solubility of calcite. Here we use experimental data (Ellis, 1963; Malinin and Kanukov, 1971; Nagy, 1988; Wolf et al., 1989), which were not employed in the model parameterization, to verify our model. It is remarkable that the calcite solubility various NaCl concentrations are accurately predicted by comparing our model with the data of (Ellis, 1963), ,as shown by Fig. 7. It can be seen that the calcite solubility will increase with NaCl concentrations at least up to 1.2 m of NaCl. In fact, calcite solubility will increase with NaCl up to 2 m of NaCl as shown by Fig. 8. However, after NaCl surpasses 2 m, the calcite solubility will decrease with the increase of NaCl. Fig. 8(b), (d) and (f) indicate that our model predicts this behavior very well. The accurate prediction of our model demonstrates that our theoretical approach is well based, considering the data was not included in the parameterization. Malinin and Kanukov (1971) reported the solubility of calcite in brines under different CO_2 concentrations. Fig. 9 shows the solubility of calcite change with concentration of m_{NaCl} at fixed TP. It can be seen that the total dissolved calcium will increase with the dissolved CO_2. Fig. 10 shows comparison between this model and other models with experimental data. We find that our model can reproduce experimental data with small deviation (<5%). But others yields obvious deviations from experimental data.

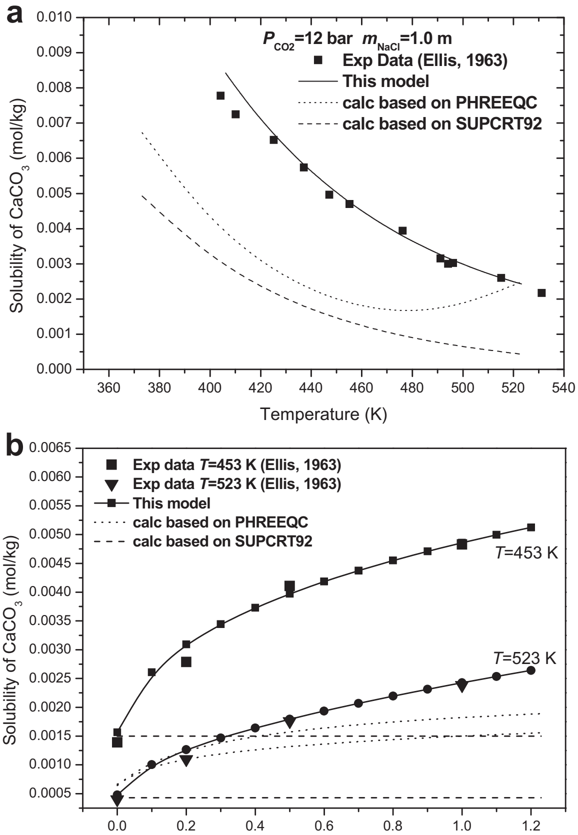

Fig. 10. Comparison between this model and other models (SUPCRT92 and PHREEQC) with experimental data. As shown in the figure, SUPCRT92 and PHREEQC deviate substantially from experimental data of Ellis (1963) in the NaCl solutions, and our model reproduces experimental data with small deviation (<5%).

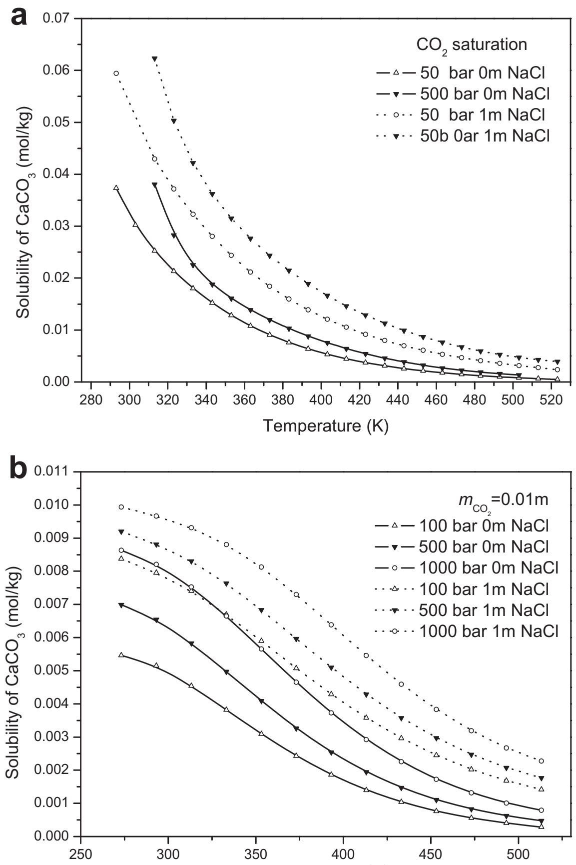

Fig. 11. The functionality of calcite solubility as a function of temperature, pressure and NaCl concentrations. The figure displays a comparison between 1.0 m NaCl (dotted lines) and 0 m NaCl (solid lines). (a) CO_2 is saturated with CO_2 vapor; (b) CO_2 molality is 0.01 mol/kg. Solubility of calcite decreased with temperature but increases sharply with pressure in low temperatures (300–400 K) or slowly in the high temperature range (above 450 K) when CO_2 is saturated. As temperature rises, dissociation of carbonate acid will become weaken (Li and Duan, 2007), so the lower acidity will make solubility of calcite decrease. Similarly, solubility of calcite will increase with increasing pressure when CO_2 concentration is fixed (0.01 m) in aqueous solution, this is because the dissociation of carbonate acid will be stronger as pressure increases.

3.1.3. Factors controlling calcite solubility

From what we discussed above, we can summarize the controlling factors for the solubility of calcite, including temperature, pressure, NaCl and CO_2 concentrations. As can be seen from Fig. 11(a) and (b) that calcite solubility will decrease with temperature, For example, at 500 bar, a temperature increases from 320 to 500 K will markedly decreases calcite solubility from 0.03 to 0.0013 mol/kg in pure water and decreases from 0.05 to 0.004 mol/kg in 1.0 m NaCl aqueous solutions. The calcite solubility is also significantly affected by pressure. With the increase of pressure, calcite solubility will increase almost linearly. However, the increased CO_2 solubility due to pressure will also cause more calcite to dissolve. In order to distinguish the effect of pressure from the effect of the dissolved CO_2, we calculated the solubility under various pressures with fixing CO_2 concentration, which is shown in Fig. 11(b). It can be seen that from Figs. 11(b) and 12 that the calcite solubility will increase with pressure. As discussed above, dissolved CO_2 will cause calcite to dissolve. Adding up to 2 m of $NaCl_{(aq)}$ will increase the solubility of calcite, but with $NaCl_{(aq)}$ concentration increases above 2 m, the calcite solubility will decrease. Fig. 13 shows predicted solubility of calcite as function of CO_2 concentration in different temperature and pressure. We can find that aqueous CO_2 concentration affects calcite solubility obviously.

3.2. Halite solubility and CO_2 solubility

CO_2 solubility and halite solubility can be calculated from this model. In previous studies (Duan and Sun, 2003, Duan et al., 2006), CO_2 solubility has been modeled

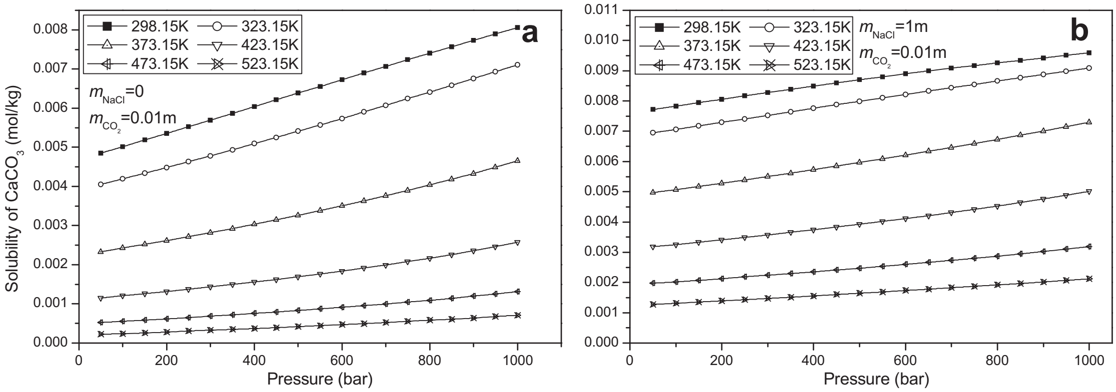

Fig. 12. Prediction of calcite solubility as function of pressure at different temperatures shows a comparison between 1.0 m NaCl (dotted lines) and 0 m NaCl (solid lines). In order to illustrate the pressure effect on calcite solubility, we fix the CO_2 concentration at 0.01 mol/kg in aqueous solution. It can be seen that the pressure increasing conduces to the solubility of calcite linearly in the *TP* range of 50–1000 bar and 298–523 K, and the slope is about 0.08–0.25 mmol/kg $CaCO_3$ per 100 bar.

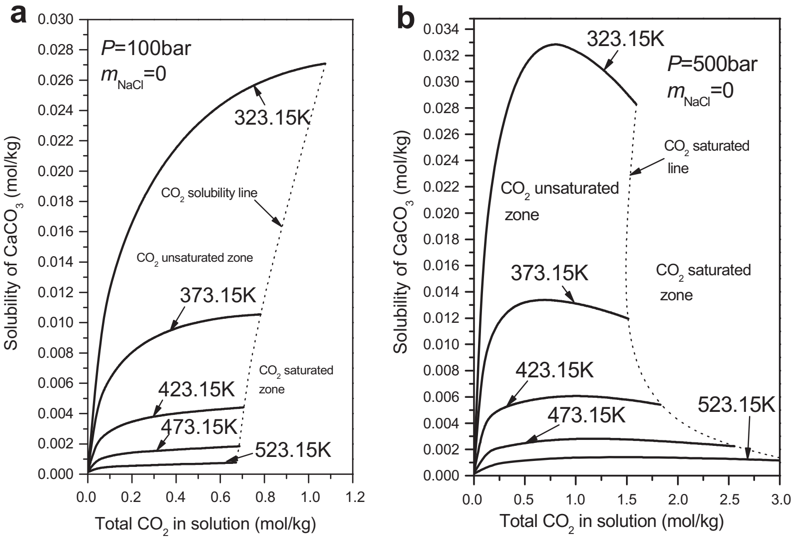

Fig. 13. Shows predicted solubility of calcite as a function of CO_2 concentration at different temperatures and pressures. Dotted line is CO_2 saturated line or CO_2 solubility line. The solubility of calcite generally increases with $CO_{2(aq)}$, but at low temperature and high pressure (323.15 K and 500 bar), calcite solubility may decrease when CO_2 concentration is lager than 1.0 mol/kg.

up to 4.5 mol/kg of NaCl. The model of this study increases the upper limit of NaCl from 4.5 m to the saturation of halite with same high accuracy as the previous models. In the presence of CO_2 and calcium species in solution, halite solubility shifts from that in pure water. It can be seen from Fig. 14 that adding $CO_{2(aq)}$ in the solution will make halite less soluble. Experimentally it is difficult to measure gas (CO_2)–water(H_2O)–solid(halite and calcite) system phase equilibrium, but we can predict the equilibrium with this model with confidence as shown in Fig. 15. Fig. 16 shows that $CaCO_3$ has little effect on the solubility of CO_2 because of its very low saturated concentration.

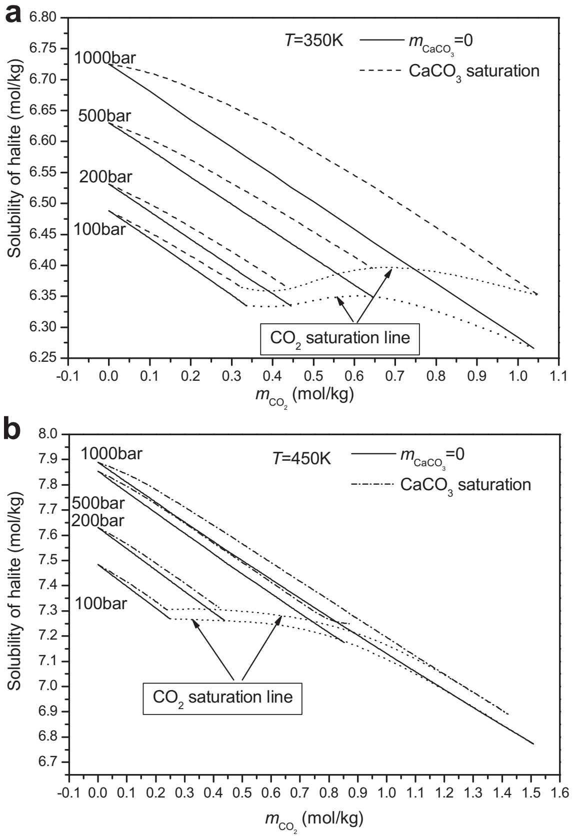

Fig. 14. Solubility of halite in aqueous solution is shown as function of concentration of CO_2. It can be seen that halite solubility will decrease with CO_2 concentration.

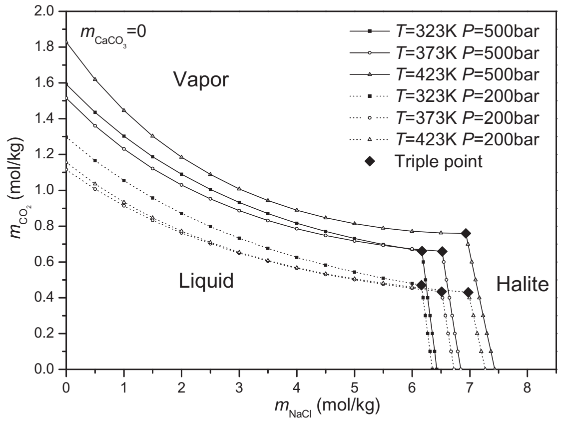

Fig. 15. CO_2 and halite solubility. We can find that m_{CO_2} is a function of m_{NaCl} at condition of NaCl unsaturation, and m_{NaCl} is a function of m_{CO_2} at condition of CO_2 unsaturation. S points in the figure are triple points, where gas–water–solid will coexist.

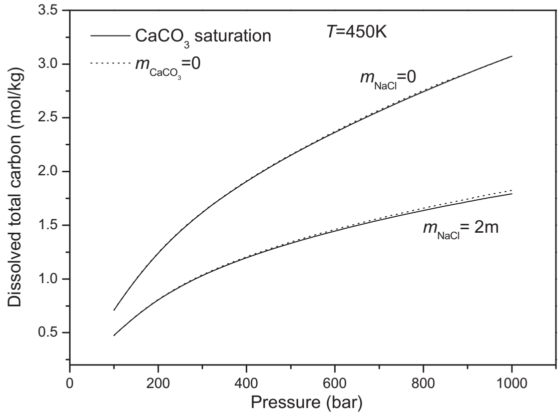

Fig. 16. The total dissolved carbon in aqueous solution is shown as a function of pressure. There is little difference between $CaCO_3$ undersaturation and $CaCO_3$ saturation, because $CO_{2(\ aq)}$, bicarbonate and carbonate are the major species of carbon in aqueous solution, and the effect from $CaCO_3$ dissolving is very limited.

3.3. Alkalinity

In general, alkalinity or A_T is a measure of the ability of a solution to neutralize acids to the equivalence point of carbonate or bicarbonate. The alkalinity is equal to the stoichiometric sum of the bases in solution. In the natural environment, carbonate alkalinity tends to make up most of the total alkalinity due to the common occurrence and

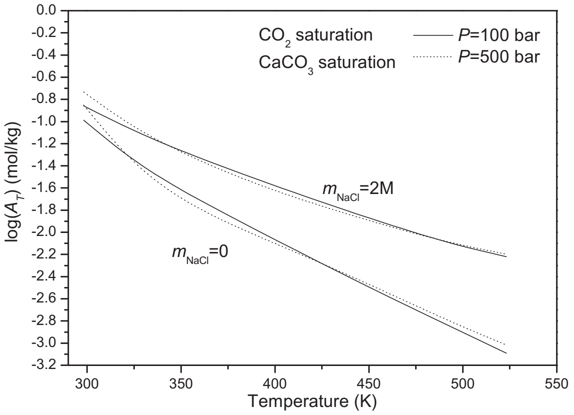

Fig. 17. Predicted negative logarithm of total alkalinity of aqueous solution as function of temperature at different pressures and m_{NaCl} conditions. We can see from this figure that there is little deviation of the alkalinity between 100 and 500 bar even though CO_2 solubility increases. This is because $CaCO_3$ can dissolve into solution as a buffer.

dissolution of carbonate rocks and presence of carbon dioxide in system. In this study, we define the alkalinity as.

$$A_T = [\mathrm{HCO_3^-}] + 2[\mathrm{CO_3^{2-}}] + [\mathrm{OH^-}] - [\mathrm{H^+}] \qquad (44)$$

Because this model employed method of coupled phase and aqueous species equilibrium, we can compute the molality of every species in aqueous solution which include the molalities of HCO_3^-, CO_3^{2-}, OH^- and H^+ by given initial condition. So it is obvious that alkalinity can been calculated from sum of these molalities based on Eq. (44). As shown in Fig. 17 that alkalinity decreases with temperature, and increases with NaCl. The pressure effect is very small.

3.4. pH value

In general, pH value is defined as negative logarithm of activity of H^+ ion. Using this model, we can predict pH value at some initial *TPm* condition. Fig. 18 shows the result by using this model to predict pH value of CO_2 saturated aqueous solution. We find the pH value will decrease with increasing temperature and pressure. pH value of aqueous solution at $CaCO_3$ saturation is higher than that at $m_{CaCO_3} = 0$ condition obviously. In this case, we think that calcite works as buffer of pH value. Coexisting calcite in the system will prevent pH value drop quickly when CO_2 drop into aqueous solution.

3.5. Distribution of calcium species

There are three kinds of calcium species (Ca^{2+}, $CaHCO_3^+$ and $CaCO_3^0$ in the aqueous solution when calcite is dissolved. Using this model, we can predict the distribution of calcium species at some initial *TPm* condition. Fig. 19 shows the result from this model prediction. We can find that Ca^{2+} and $CaHCO_3^+$ are main calcium species in aqueous solution. However, the species of $CaCO_3^0$ accounts for very little under most conditions.

4. CONCLUSIONS

We have developed a thermodynamic model of coupled phase and aqueous species equilibrium in the H_2O–CO_2–NaCl–$CaCO_3$ system from 0 to 250 °C, 1 to 1000 bar up to saturation of halite. From this model, calcite solubility, species concentrations, CO_2 solubility, pH, alkalinity and liquid–vapor–solid equilibrium, can be accurately calculated. Compared to previous models, this model covers much larger *T*–*P*–*m* space and is more reliable, especially in the elevated pressure and high molality of NaCl region. The merit and advantage of this model is its predictability, the model was not constructed by fitting these experimental data.

As calculated from this model, calcite solubility is a function of temperature, pressure, $CO_{2(aq)}$ concentration

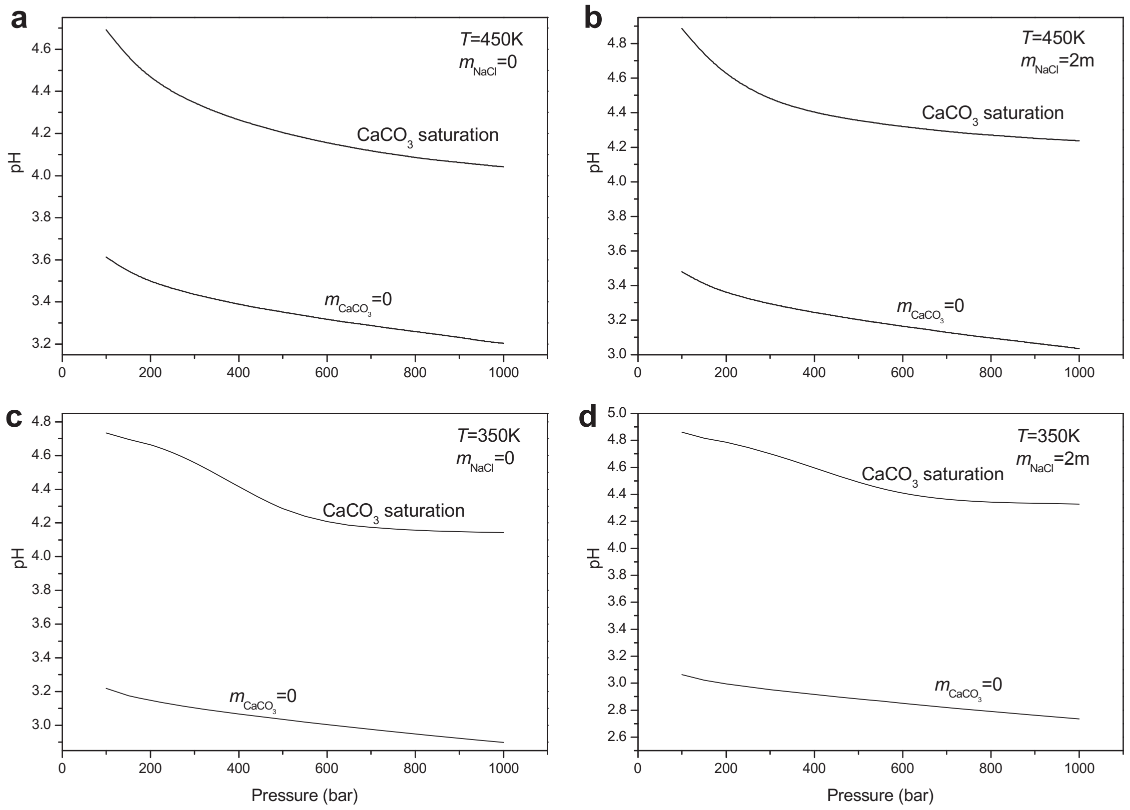

Fig. 18. Model prediction of pH values in CO_2 saturated aqueous solutions. We find that the pH value will decrease with temperature and pressure and that pH value in $CaCO_3$ saturation solutions is much higher than that in the solution with no $CaCO_3$, which is resulted from the formation of $CaHCO_3^+$ when calcite dissolve into aqueous solution.

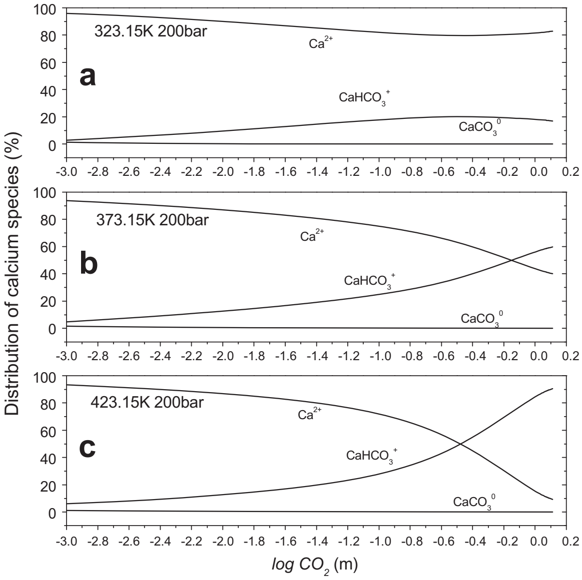

Fig. 19. There are three kinds of calcium species (Ca^{2+}, $CaHCO_3{}^{+}$, $CaCO_3{}^{0}$) in the aqueous solution when calcite is dissolved. Distribution of calcium species is shown in this figure. Ca^{2+} is the most species in low CO_2 concentration and low temperature, and its percent ratio will decrease with adding CO_2 into solution, $CaHCO_3{}^{+}$ accounts for the second abundant species in low CO_2 concentrations and low temperatures, but its percentage will increase with adding CO_2 into solution and become the most abundant species at high temperatures and high CO_2 concentrations (at 373.15 K $\log(m_{CO_2}) = -0.15$ and at 473.15 K $\log(m_{CO_2}) = -0.45$). $CaCO_3{}^{0}$ accounts for only a small percentage under any conditions.

and NaCl concentration. (1) As temperature increases, calcite solubility decreases. For example, when temperature increases from 273 to 373 K, calcite solubility decreases by about 50%; (2) with the increase of pressure, calcite solubility increases. For example, at 373 K changing pressure from 10 bar to 500 bar may increase calcite solubility by about 30%; (3) dissolved CO_2 in solution is an essential factor to control calcite–liquid phase equilibrium. Very little dissolved CO_2 can increase calcite solubility substantially. (4) increasing concentration of NaCl up to 2 m will increase the solubility of calcite, but further increasing NaCl solubility beyond 2 m will decrease the solubility of calcite.

pH value, alkalinity, CO_2 solubility the concentration of many aqueous species are all functions of temperature, pressure and $NaCl_{(aq)}$ concentrations. Their functionality can be found from the application of this model. Online calculation is made available on www.geochem-model.org/models/h2o_co2_nacl_caco3/calc.php.

ACKNOWLEDGMENTS

This work is supported by Zhenhao Duan's "Major development Funds" (code #: kzcx2-yw- 124) by Chinese Academy of Sciences, the "Key Project Funds" (No. 40537032) by National Science Foundation of China and Wenxun Hu's 973 funds CompanySupported by the NKBRDPC (Grant No.2005CB422103) and his funds (40673040) supported by NSFC, and the 973 Project Funds (#2006CB-705800) awarded by the Ministry of Science and Technology of China. We thank Drs. Eric Oelkers, Leonid Aranovichi and two anonymous reviewers for the constructive suggestions for improving the paper.

APPENDIX A. THE ION PRODUCT OF WATER

The empirical model to calculate ion product of water developed by Marshall and Franck (1981) has the following form:

$$\log K_w = A + B/T + C/T^2 + D/T^3 + (E + F/T + G/T^2)\log \rho_w \tag{A1}$$

where K_w is ion product of water with the unit of $(mol/kg)^2$, ρ_w is density of water (in g/cm^3), which can be deduced from the equation of state for H_2O developed by Wagner and Kruse (1998) and T is temperature in K. The parameters, A–G, are listed in Table A1.

APPENDIX B. THE EMPIRICAL MODEL FOR THE SOLUBILITY OF HALITE AND DISSOCIATION CONSTANT IN WATER

The empirical model to calculate solubility of halite in water has the following form:

$$\ln m_s = \ln(a_1 + a_2T + a_3T^2) + \theta(P + \omega P^2 - 1) \tag{B1}$$

where T is temperature in K and P is pressure in bar and ms is solubility of NaCl in water with the unit of mol/kg. The parameters of Eq. (B1), a_1–a_3, θ and ω are also listed in Table B1. This model can be employed safely in the range of 273.15–573.15 K and 1–2000 bar. The main references are (Adams, 1931; Linke and Seidell, 1958; Stephen and Stephen, 1963; Vanhook, 1980; Pinho and Macedo, 2005).

In this study, we set activity coefficient of halite, a_{NaCl}, as unit, so

$$K_9 = (m_{Na^+}\gamma_{Na^+}) \cdot (m_{Cl^-}\gamma_{Cl^-}) = m_s\gamma_{Na^+}\gamma_{Cl^-} \tag{B2}$$

where m_s is halite solubility and it can be calculated by Eq. (B1); γ_{Na^+} and γ_{Cl^-} are activity coefficients of Na^+ and Cl^-

Table A1
Parameters for Eq. (A1)

A	−4.098
B	−3245.2
C	2.2362e+5
D	−3.984e+7
E	13.957
F	−1262.3
G	8.5641e+5

Table B1
Parameters for Eq. (B1)

a_1	8.316
a_2	−1.843e−02
a_3	3.757e−05
θ	4.6e−05
ω	−2.2e−04

Table B2
Parameters for Eq. (B3)

a_1	1.188919e+03
a_2	−2.636581e+00
a_3	−1.561700e+05
a_4	+1.795657e−03
A_5	+3.237887e−03
a_6	+5.409459e−05
a_7	+7.200665e−06
a_8	−2.992790e−08

in aqueous solution, respectively, and they are functions of TPm_s. We can use Pitzer model to calculate their values at fixed TPm_s (Pitzer et al., 1984). So we obtain K_9 value in the interested TP range, and fit it as a polynomial equation:

$$K_9 = a_1 + a_2T + a_3/T + a_4T^2 + a_5P + a_6TP + a_7P^2 + a_8TP^2 \tag{B3}$$

where a_1 to a_8 are parameters which are shown in Table B2.

REFERENCES

Adams L. H. (1931) Equilibrium in binary systems under pressure. I. An experimental and thermodynamic investigation of the system, NaCl–H_2O, at 25 °C. *J. Am. Chem. Soc.* **53**, 3769–3813.

Allison J. D., Brown D. S. and Novo-Gradac K. J. (1991) MINTEQA2/PRODEFA2, A Geochemical Assessment Model for Environmental Systems: Version 3.0 User's Manual. EPA 600-3-91021. Environmental Research Laboratory Office of Research and Development U.S. Environmental Protection Agency Athens, Georgia 30605.

Anderson G. M., Castet S., Schott J. and Mesmer R. E. (1991) The density model for estimation of thermodynamic parameters of reactions at high-temperatures and pressures. *Geochim. Cosmochim. Acta* **55**(7), 1769–1779.

Anderson G. M. and Crerar D. A. (1993). *Thermodynamics in Geochemistry. The Equilibrium Model*. Oxford University Press.

Ball J. W. and Nordstrom D. K. (1991) User's manual for WATEQ4F, with revised thermodynamic database and test cases for calculating speciation of major, trace and redox elements in natural waters. Open-File Report 91-183. U.S. Geological Survey.

Bates R. G., Bower V. E., Canham R. G. and Prue J. E. (1959) The dissociation constant of $CaOH^+$ from 0 to 40 °C. *Trans. Faraday Soc.* **55**(12), 2062–2068.

Berendsen P. (1971) The solubility of calcite in carbon-dioxide–water solutions, from 100 to 300 °C, 100 to 1000 bars, and 0 to 10 weight per cent CO_2, and geologic applications. Ph.D. dissertation, University of California, Riverside.

Bischoff J. L. (1969) Temperature controls on aragonite–calcite transformation in aqueous solution. *Am. Mineral.* **52**(1–2), 149–155.

Blencoe J. G., Naney M. T. and Anovitz L. M. (2001) The CO_2–H_2O system: III. A new experimental method for determining liquid–vapor equilibria at high subcritical temperatures. *Am. Mineral.* **86**(9), 1100–1111.

Caciagli N. C. and Manning C. E. (2003) The solubility of calcite in water at 6–16 kbar and 500–800 °C. *Contrib. Mineral. Petrol.* **146**(3), 275–285.

Christov C. and Møller N. (2004a) A chemical equilibrium model of solution behavior and solubility in the H–Na–K–Ca–OH–Cl–HSO_4–SO_4–H_2O system to high concentration and temperature. *Geochim. Cosmochim. Acta* **68**(18), 3717–3739.

Christov C. and Møller N. (2004b) Chemical equilibrium model of solution behavior and solubility in the H–Na–K–OH–Cl–HSO_4–SO_4–H_2O system to high concentration and temperature. *Geochim. Cosmochim. Acta* **68**(6), 1309–1331.

Dorange G., Marchand A. and Guyader M. L. (1990) Produit de solubilite de la calcite et constantes de dissociation de $CaHCO_3^+$ et $CaCO_3^0$ entre 5 et 75 °C. *Rev. Sci.* **3**, 261–275.

Duan Z., Møller N. and Weare J. H. (1992) An equation of state for the CH_4–CO_2–H_2O system: I. Pure systems from 0 to 1000 °C and 0 to 8000 bar. *Geochim. Cosmochim. Acta* **56**(7), 2605–2617.

Duan Z. and Sun R. (2003) An improved model calculating CO_2 solubility in pure water and aqueous NaCl solutions from 273 to 533 K and from 0 to 2000 bar. *Chem. Geology* **193**(3–4), 253–271.

Duan Z., Sun R., Zhu C. and Chou I-Min (2006) An improved model for the calculation of CO_2 solubility in aqueous solutions containing Na^+, K^+, Ca^{2+}, Mg^{2+}, Cl^-, and SO_4^{2-}. *Marine Chem.* **98**(2–4), 131–139.

Duan Z., Hu J., Li D. and Mao S. (2008) Densities of the CO_2-H_2O and CO_2-H_2O-NaCl Systems Up to 647 K and 100 MPa. *Energy & Fuels* **22**(3), 1666–1674.

Ellis A. J. (1959) The solubility of calcite in carbon dioxide solutions. *Am. J. Sci.* **257**(5), 354–365.

Ellis A. J. (1963) Solubility of calcite in sodium chloride solutions at high temperatures. *Am. J. Sci.* **261**(3), 259–267.

Frantz J. D. and Marshall W. L. (1982) Electrical conductances and ionization-constants of calcium-chloride and magnesium-chloride in aqueous-solutions at temperatures to 600 °C and pressures to 4000 bars. *Am. J. Sci.* **282**(10), 1666–1693.

Fresenius R. (1846) Ueber die Löslichkeitsverhältnisse von einigen, bei der quantitativen Analyse als Bestimmungsformen etc. dienenden Niederschlägen. *Ann. Chem. Pharm.* **59**(1), 117.

Garcia J. E. (2001) Density of aqueous solutions of CO_2. Lawrence Berkeley National Laboratory. Paper LBNL-49023. http://www.repositories.cdlib.org/lbnl/LBNL-49023.

Giles M. R. (1987) Mass transfer and problems of secondary porosity creation in deeply buried hydrocarbon reservoirs. *Mar. Petrol. Geol.* **4**(3), 188–204.

Giles M. R. and de Boer R. B. (1989) Secondary porosity: creation of enhanced porosities in the subsurface from the dissolution of carbonate cements as a result of cooling formation waters. *Mar. Petrol. Geol.* **6**(3), 261–269.

Gillespie S. E., Oscarson J. L., Chen X., Izatt R. M. and Pando C. (1992) Thermodynamic quantities for the interaction of Cl^- with Mg^{2+}, Ca^{2+} and H^+ in aqueous-solution from 250 to 325 °C. *J. Solut. Chem.* **21**(8), 761–788.

Gimblett F. G. R. and Monk C. B. (1954) Emf studies of electrolytic dissociation.7. Some alkali and alkaline earth metal hydroxides in water. *Trans. Faraday Soc.* **50**(9), 965–972.

Greenberg J. P. and Møller N. (1989) The prediction of mineral solubilities in natural waters: a chemical equilibrium model for the Na–K–Ca–Cl–SO_4–H_2O system to high concentration from 0 to 250 °C. *Geochim. Cosmochim. Acta* **53**(10), 2503–2518.

Greenwald I. (1941) The dissociation of calcium and magnesium carbonates and bicarbonates. *J. Biol. Chem.* **141**(3), 789–796.

Gu Y., Gammons C. H. and Bloom M. S. (1994) A one-term extrapolation method for estimating equilibrium-constants of aqueous reactions at elevated-temperatures. *Geochim. Cosmochim. Acta* **58**(17), 3545–3560.

Harvie C. E., Møller N. and Weare J. H. (1984) The prediction of mineral solubilities in natural waters: the Na–K–Mg–Ca–H–Cl–SO_4–OH–HCO_3–CO_3–CO_2–H_2O system to high ionic strengths at 25 °C. *Geochim. Cosmochim. Acta* **48**(4), 723–751.

Harvie C. E. and Weare J. H. (1980) The prediction of mineral solubilities in natural waters: the Na–K–Mg–Ca–Cl–SO_4–H_2O

system from zero to high concentration at 25 °C. *Geochim. Cosmochim. Acta* **44**(7), 981–997.

Helgeson H. C. (1969) Thermodynamics of hydrothermal systems at elevated temperatures and pressures. *Am. J. Sci.* **267**(7), 729–804.

Jacobson R. L. and Langmuir D. (1974) Dissociation-constants of calcite and $CaHCO_3^+$ from 0 to 50 °C. *Geochim. Cosmochim. Acta* **38**(2), 301–318.

Johnson J. W., Oelkers E. H. and Helgeson H. C. (1992) SUPCRT92: a software package for calculating the standard molal thermodynamic properties of minerals, gases, aqueous species, and reactions from 1 to 5000 bar and 0 to 1000 °C. *Comput. Geosci.* **18**(7), 899–947.

Lassaigne J. L. (1848) Löslichkeit einiger kohlensauren Salze in kohlensaurem Wasser. *Ann. Chem. Pharm.* **68**(2), 253.

Li D. and Duan Z. (2007) The speciation equilibrium coupling with phase equilibrium in the H_2O–CO_2–NaCl system from 0 to 250 °C, from 0 to 1000 bar, and from 0 to 5 molality of NaCl. *Chem. Geol.* **244**(3–4), 730–751.

Li L., Peters C. A. and Celia M. A. (2007) Effects of mineral spatial distribution on reaction rates in porous media. *Water Resour. Res.* **43**(1).

Linke W. F. and Seidell A. (1958) *Solubilities of Inorganic and Metal Organic Compounds*. American Chemical Society, Washington, DC.

Malinin S. D. and Kanukov A. B. (1971) Solubility of calcite in homogeneous H_2O–NaCl–CO_2 systems in 200–600 °C temperature interval. *Geochem. Int. USSR* **8**(5), 668–679.

Marshall W. L. and Franck E. U. (1981) Ion product of water substance, 0–10,000 °C, 1–10,000 bars new international formulation and its background. *J. Phys. Chem. Ref. Data* **10**(2), 295–304.

Martynov O. I., Vasina L. G. and Pozdnyak S. (1972) Determination of dissociation-constants of ion pairs $CaOH^+$, $CaHCO_3^+$, and $CaCO_3^0$ over the temperature range 22–98 °C. *Dokl. Akad. Nauk SSSR* **202**(6), 1337–1340.

Martynov O. I., Vasina L. G. and Pozdnyak S. (1971) Determination of solubility product of calcium carbonate in 22–98 °C temperature range. *Dokl. Akad. Nauk SSSR* **201**(5), 1110–1113.

Medeiros S. K., Albuquerque E. L., Maia J. F. F., Caetano E. W. S. and Freire V. N. (2007) First-principles calculations of structural, electronic, and optical absorption properties of $CaCO_3$ vaterite. *Chem. Phys. Lett.* **435**(1–3), 59–64.

Mesmer R. E., Marshall W. L., Palmer D. A., Simonson J. M. and Holmes H. F. (1988) Thermodynamics of aqueous association and ionization reactions at high-temperatures and pressures. *J. Solut. Chem.* **17**(8), 699–718.

Miller J. P. (1952) A portion of the system calcium carbonate–carbon dioxide–water, with geological implications. *Am. J. Sci.* **250**(3), 161–208.

Moore E. W. and Verine H. J. (1981) Pancreatic calcification—formation-constants of $CaHCO_3^+$ and $CaCO_3^0$ complexes determined with Ca^{2+} electrode. *Am. J. Physiol.* **241**(2), G182–G190.

Morey G. W. (1962) The action of water on calcite, magnesite and dolomite. *Am. Mineral.* **47**, 1456–1460.

Nagy K. L. (1988) The solubility of calcite in NaCl and Na–Ca–Cl brines. Ph.D. dissertation, Texas A& M University.

Nakayama F. S. (1968) Calcium activity complex and ion-pair in saturated $CaCO_3$ solutions. *Soil Sci.* **106**(6), 429.

Nakayama F. S. (1971) Thermodynamic functions for the dissociation of $NaHCO_3^0$, $NaCO_3^-$, H_2CO_3 and HCO_3^-. *J. Inorg. Nucl. Chem.* **33**(5), 1287–1291.

Nelder J. A. and Mead R. (1965) A simplex-method for function minimization. *Comput. J.* **7**(4), 308–313.

Neuman W. F., Morrow P. E., Toribara T. Y., Casarett L. J., Mulryan B. J. and Hodge H. C. (1956) Evidence for complex ion formation in the calcium bicarbonate system. *J. Biol. Chem.* **219**(2), 551–555.

Newton R. C. and Manning C. E. (2002) Experimental determination of calcite solubility in H_2O–NaCl solutions at deep crust/upper mantle pressures and temperatures: implications for metasomatic processes in shear zones. *Am. Mineral.* **87**(10), 1401–1409.

Pabalan R. T. and Pitzer K. S. (1987) Thermodynamics of concentrated electrolyte mixtures and the prediction of mineral solubilities to high temperatures for mixtures in the system Na–K–Mg–Cl–SO_4–OH–H_2O. *Geochim. Cosmochim. Acta* **51**(9), 2429–2443.

Parkhurst D. L. and Appelo C. A. J. (1999) User's guide to PHREEQC (version 2)—a computer program for speciation, batch-reaction, one-dimensional transport, and inverse geochemical calculations. Water-Resources Investigations Report 99-4259. U.S. Geological Survey.

Pinho S. P. and Macedo E. A. (2005) Solubility of NaCl, NaBr, and KCl in water, methanol, ethanol, and their mixed solvents. *J. Chem. Eng. Data* **50**(1), 29–32.

Pitzer K. S. (1973) Thermodynamics of electrolytes. I. Theoretical basis and general equations. *J. Phys. Chem.* **77**(2), 268–277.

Pitzer K. S. and Kim J. J. (1974) Thermodynamics of electrolytes. IV. Activity and osmotic coefficients for mixed electrolytes. *J. Am. Chem. Soc.* **96**(18), 5701–5707.

Pitzer K. S. and Mayorga G. (1973) Thermodynamics of electrolytes. II. Activity and osmotic coefficients for strong electrolytes with one or both ions univalent. *J. Phys. Chem.* **77**(19), 2300–2308.

Pitzer K. S., Peiper J. C. and Busey R. H. (1984) Thermodynamic properties of aqueous sodium chloride solutions. *J. Phys. Chem. Ref. Data* **13**(1), 1–102.

Plummer L. N. and Busenberg E. (1982) The solubilities of calcite, aragonite and vaterite in CO_2–H_2O solutions between 0 °C and 90 °C, and an evaluation of the aqueous model for the system $CaCO_3$–CO_2–H_2O. *Geochim. Cosmochim. Acta* **46**(6), 1011–1040.

Plummer L. N., Parkhurst D. L., Fleming G. W. and Dunkle S. A. (1988) A computer program incorporating Pitzer's equations for calculation of geochemical reactions in brines. Water-Resources Investigations Report 88-4153. U.S. Geological Survey.

Pool K. H., Raney P. J. and Shannon D. W. (1987) Calcite solubility in simulated geothermal brines. DoE Report DE87 006589. Pacific Northwest Laboratory, Richland, Washington.

Pruess K. and Spycher N. (2007) ECO2N—a fluid property module for the TOUGH2 code for studies of CO_2 storage in saline aquifers. *Energy Convers. Manage.* **48**(6), 1761–1767.

Quist A. S. (1970) Ionization constant of water to 800 °C and 4000 bars. *J. Phys. Chem.* **74**(18), 3396–3402.

Quist A. S. and Marshall W. L. (1968) Electrical conductances of aqueous sodium chloride solutions from 0 to 800 °C and at pressures to 4000 bars. *J. Phys. Chem.* **72**(2), 684–703.

Reardon E. J. and Langmuir D. (1974) Thermodynamic properties of ion-pairs $MgCO_3^0$ and $CaCO_3^0$ from 10 to 50 °C. *Am. J. Sci.* **274**(6), 599–612.

Ruaya J. R. (1988) Estimation of instability constants of metal chloride complexes in hydrothermal solutions up to 300 °C. *Geochim. Cosmochim. Acta* **52**(8), 1983–1996.

Sass E., Morse J. W. and Millero F. J. (1983) Dependence of the values of calcite and aragonite thermodynamic solubility products on ionic models. *Am. J. Sci.* **283**(3), 218–229.

Satman A., Ugur Z. and Onur M. (1999) The effect of calcite deposition on geothermal well inflow performance. *Geothermics* **28**(3), 425–444.

Seewald J. S. and Seyfried J. W. E. (1991) Experimental determination of portlandite solubility in H_2O and acetate solutions at 100–350 °C and 500 bars: constraints on calcium hydroxide and calcium acetate complex stability. *Geochim. Cosmochim. Acta* **55**(3), 659–669.

Segnit E. R., Holland H. D. and Biscardi C. J. (1962) The solubility of calcite in aqueous solutions—I. The solubility of calcite in water between 75 °C and 200 °C at CO_2 pressures up to 60 atm. *Geochim. Cosmochim. Acta* **26**(12), 1301–1331.

Sharp W. E. and Kennedy G. C. (1965) The system CaO–CO_2–H_2O in the two-phase region calcite + aqueous solution. *J. Geol.* **73**(2), 391–403.

Shock E. L., Helgeson H. C. and Sverjensky D. A. (1989) Calculation of the thermodynamic and transport properties of aqueous species at high pressures and temperatures: standard partial molal properties of inorganic neutral species. *Geochim. Cosmochim. Acta* **53**(9), 2157–2183.

Spycher N., Pruess K. and Ennis-King J. (2003) CO_2–H_2O mixtures in the geological sequestration of CO_2. I. Assessment and calculation of mutual solubilities from 12 to 100 °C and up to 600 bar. *Geochim. Cosmochim. Acta* **67**(16), 3015–3031.

Stephen H. and Stephen T. (1963) *Solubilities of Inorganic and Organic Compounds: Binary Systems*. Perganmon Press, Oxford, England.

Sverjensky D. A., Shock E. L. and Helgeson H. C. (1997) Prediction of the thermodynamic properties of aqueous metal complexes to 1000 °C and 5 kb. *Geochim. Cosmochim. Acta* **61**(7), 1359–1412.

Tanger J. C. and Helgeson H. C. (1988) Calculation of the thermodynamic and transport-properties of aqueous species at high-pressures and temperatures—revised equations of state for the standard partial molal properties of ions and electrolytes. *Am. J. Sci.* **288**(1), 19–98.

Tanger J. C. and Pitzer K. S. (1989) Calculation of the ionization-constant of H_2O to 2,273 K and 500 MPa. *AIChE J.* **35**(10), 1631–1638.

Vanhook W. A. (1980) The pressure coefficient of solubility for some alkali-halides and its solvent isotope effect. *Fluid Phase Equilibria* **4**(3–4), 287–292.

Wagner W. and Kruse A. (1998) *Properties of Water and Steam*. Springer-Verlag, Berlin, Heidelberg.

Weyl P. K. (1959) The change in solubility of calcium carbonate with temperature and carbon dioxide content. *Geochim. Cosmochim. Acta* **17**(3–4), 214–225.

Wolf M., Breitkopf O. and Puk R. (1989) Solubility of calcite in different electrolytes at temperatures between 10 and 60 °C and at CO_2 partial pressures of about 1 kPa. *Chem. Geol.* **76**(3–4), 291–301.

Associate editor: Eric H. Oelkers